A Report on Research Sponsored by
NATIONAL SCIENCE FOUNDATION
(RANN)
Grant No. ENV74-14766

STRUCTURAL WALLS IN EARTHQUAKE-RESISTANT BUILDINGS

Dynamic Analysis Of Isolated Structural Walls

INPUT MOTIONS

by

Arnaldo T. Derecho
L. Erik Fugelso
Mark Fintel

Submitted by
RESEARCH AND DEVELOPMENT
CONSTRUCTION TECHNOLOGY LABORATORIES
PORTLAND CEMENT ASSOCIATION
5420 Old Orchard Road
Skokie, Illinois 60076
December 1977

50272-101

REPORT DOCUMENTATION PAGE	1. REPORT NO. NSF/RA-780200	2.	3. Recipient's Accession No. PB 288028

4. Title and Subtitle Structural Walls in Earthquake-Resistant Buildings, Dynamic Analysis of Isolated Structural Walls - Input Motions, Final Report	5. Report Date December 1977
	6.
7. Author(s) A.T. Derecho, L.E. Fugelso, M. Fintel	8. Performing Organization Rept. No. PCA R/D Ser. 1586
9. Performing Organization Name and Address Portland Cement Association 5420 Old Orchard Road Skokie, Illinois 60076	10. Project/Task/Work Unit No. 11. Contract(C) or Grant(G) No. (C) (G) ENV7414766
12. Sponsoring Organization Name and Address National Science Foundation Division of Advanced Technology Applications Washington, D.C. 20550	13. Type of Report & Period Covered Final 14.

15. Supplementary Notes

16. Abstract (Limit: 200 words)

A characterization of input motions for use in dynamic analysis is given in terms of intensity, duration and frequency content. Different measures of intensity are examined. On the basis of this examination, spectrum intensity is selected as a good measure of ground motion intensity. A review of the work of other investigators shows that a 20-second duration of strong ground motion is generally adequate for determining maximum cumulative deformation estimates of maximum response quantities other than cumulative deformations. Estimates of maximum response may be obtained using 10 seconds of strong ground motion. Accelerograms are classified with respect to frequency content as "peaking" or "broad band", depending upon the character of the associated 5%-damped relative velocity response spectra.

17. Document Analysis a. Descriptors

Earthquakes	Intensity	Earthquake resistant structures
Seismic waves	Dynamic structural analysis	Design criteria
Critical frequencies	Dynamic response	

b. Identifiers/Open-Ended Terms

c. COSATI Field/Group

18. Availability Statement	19. Security Class (This Report)	21. No. of Pages
NTIS		59
	20. Security Class (This Page)	22. Price

(See ANSI–Z39.18) See Instructions on Reverse OPTIONAL FORM 272 (4–77) (Formerly NTIS–35) Department of Commerce

CAPITAL SYSTEMS GROUP, INC.
6110 EXECUTIVE BOULEVARD
SUITE 250
ROCKVILLE, MARYLAND 20852

TABLE OF CONTENTS

Page No.

SYNOPSIS i

BACKGROUND 1

INTRODUCTION 5

CHARACTERIZATION OF INPUT MOTIONS 7

Duration of Input Motion 7

Frequency Characteristics of Input Motion 8

Classification of Accelerograms 10

Frequency Content and Structural Response 11

Inventory of Acceleration Records 12

Intensity of Input Motions 14

Spectrum Intensity vs. Ductility of SDF Systems . 15

SUMMARY 19

REFERENCES 21

ACKNOWLEDGMENTS 25

TABLES 27

FIGURES 31

APPENDIX 41

SYNOPSIS

Although structural walls have a long history of satisfactory use in stiffening buildings against wind, there is insufficient information on their behavior under strong earthquakes. Observations of the performance of buildings during recent earthquakes have demonstrated the superior performance of buildings stiffened by properly proportioned and designed structural walls from the point of view of safety and especially from the standpoint of damage control.

The primary objective of the analytical investigation, of which the work reported here is a part, is the estimation of the maximum forces and deformations that can reasonably be expected in critical regions of structural walls subjected to strong ground motion. The results of the analytical investigation, when corrolated with data from the concurrent experimental program, will form the basis for the design procedure that is to be developed as the ultimate objective of the overall investigation.

This is the first part of the report on the analytical investigation. It deals mainly with the characterization of input motions in terms of intensity, duration and frequency content. Accelerograms are classified with respect to frequency content as "peaking" or "broad band" depending upon the character of the associated velocity response spectra. It is shown that "spectrum intensity" is a good measure of ground motion intensity. The main purpose of the characterization is to enable the determination of maximum or critical dynamic response using the least number of input motions in the analyses.

Dynamic Analysis Of Isolated Structural Walls

INPUT MOTIONS

by

A. T. Derecho[(1)], L. E. Fugelso[(2)], and M. Fintel[(3)]

BACKGROUND

Although structural walls* have a long history of satisfactory use in stiffening multistory buildings against wind, not enough information is available on the behavior of such elements under strong earthquake conditions.

Observations of the performance of buildings subjected to earthquakes during the past decade have focused attention on the need to minimize damage in addition to ensuring the general safety of buildings during strong earthquakes. The need to control damage to structural and nonstructural components during earthquakes becomes particularly important in hospitals and other facilities that must continue operation following a major disaster. Damage control, in addition to life safety, is also economically desirable in tall buildings designed for residential and commercial occupancy, since the non-structural components in such buildings usually account for 60 to 80 percent of the total cost.

There is little doubt that structural walls offer an efficient way to stiffen a building against lateral loads. When proportioned so that they possess adequate lateral stiffness to reduce interstory distortions due to earthquake-induced

(1)Manager, Structural Analytical Section, Engineering Development Department, (2)Formerly, Structural Engineer, Design Development Section, and (3)Director, Advanced Engineering Services, Portland Cement Association, Skokie, Illinois.

*In conformity with the nomenclature be adopted by the Applied Technology Council (1) and in the forthcoming revised edition of Appendix A to ACI 318-71,"Building Code Requirements for Reinforced Concrete", (2), the term "structural wall" is used in place of "shear wall".

motions, walls effectively reduce the likelihood of damage to the nonstructural elements contained in a building. When used with rigid frames, walls form a structural system that combines the gravity-load-carrying efficiency of the rigid frame with the lateral-load-resisting efficiency of the structural wall.

Observations of the comparative performance of rigid frame buildings and buildings stiffened by structural walls during recent earthquakes,[3,4,5] have clearly demonstrated the superior performance of buildings stiffened by properly proportioned structural walls. Performance of the structural wall buildings was better both from the point of view of safety and from the standpoint of damage control.

The need to minimize damage during strong earthquakes, in addition to the primary requirement of life safety (i.e., no collapse), clearly imposes more stringent requirements on the design of structures. This need to minimize damage provided the impetus for a closer examination of the structural wall as an earthquake-resisting element. Among the more immediate questions to be answered before a rational design procedure can be developed are:

1. What magnitudes of deformation and associated forces can reasonably be expected at critical regions of structural walls corresponding to specific combinations of structural and ground motion parameters? How many cycles of large deformations can be expected in critical regions of walls under earthquakes of average duration?
2. What stiffness and strength should structural walls in typical building configurations have relative to the expected ground motion in order to limit the deformations to acceptable levels?
3. What design and detailing requirements must be met to provide walls with the strength and deformation capacities indicated by analysis?

The combined analytical and experimental investigation of which this study is a part was undertaken to provide answers to the above questions. The objective of the overall investigation is the development of practical and reliable design procedures for earthquake-resistant structural walls and wall systems.

The analytical program undertaken to accomplish part of the desired objective consists of the following steps:

(a) Characterization of input motions in terms of the significant parameters to enable the calculation of critical or "near-maximum" response using a minimum number of input motions[6].

(b) Determination of the relative influence of the various structural and ground motion parameters on dynamic structural response through parametric studies[7]. The purpose of this investigation is to identify the most significant variables.

(c) Calculation of estimates of strength and deformation demands in critical regions of structural walls as affected by the significant parameters determined in Step (b). A number of input accelerograms chosen on the basis of information developed in Steps (a) and (b) are used[8].

(d) Development of procedures for determining design force levels[8] by correlating the stiffness, strength and deformation demands obtained in Step (c) with the corresponding capacities determined from the concurrent experimental program[9].

Another important result of the analytical investigation is the determination of a representative loading history[10] The loading history selected can be used in the testing of laboratory specimens under slowly reversing loads.

The first phase of this investigation is concerned mainly with isolated structural walls. A detailed consideration of the dynamic response of frame-wall and coupled wall structures is planned for the subsequent phases of the investigation.

This is the first part of the report on the analytical investigation. It deals mainly with the characterization of input motions in terms of duration, intensity and frequency content, with particular regard to the effects of these parameters on dynamic inelastic response. The material presented here is based on Part A of Reference[7].

The investigation has been supported in major part by Grant No. ENV74-14766 from the National Science Foundation, RANN Program. Any opinions, findings and conclusions expressed in this report are those of the authors and do not necessarily reflect the views of the National Science Foundation.

INTRODUCTION

The primary objective of the analytical program is to estimate the maximum forces and deformations that can be reasonably expected at critical regions in structural walls subjected to strong earthquakes. The first step in the investigation was to select an appropriate set of acceleration records to serve as horizontal base motion inputs in the dynamic analysis.

The stochastic character of structural response to earthquake motions requires consideration of a sufficient number of input motions in the dynamic analysis. To minimize the number of records that need be considered in the analysis, an examination was made of the major parameters characterizing strong-motion accelerograms. By classifying accelerograms into fairly broad categories according to certain basic properties, it should be possible to obtain good estimates of the maximum response of structures to earthquakes using a limited number of input motions.

For this work 20 records were selected from a compilation of digitized stong-motion accelerograms published by the California Institute of Technology[11]. In addition to natural records, a number of artificially generated accelerograms were considered.

The principal ground motion characteristics affecting dynamic structural response are intensity, duration and frequency content. Intensity provides a characteristic measure of the amplitude of the acceleration record. Duration refers to the length of the record during which relatively large amplitude pulses occur, with due allowance for a reasonable build-up time. The frequency characteristics of a given ground motion have to do with the relative energy content of the component waves, of different frequencies, that make up the motion.

Guzman, Crouse and Jennings[12] have pointed out that the best available indicators of the damage capability of the ground motion from earthquakes are duration and the response spectrum. The response spectrum inherently reflects the effects of intensity and frequency content, though not necessarily the duration, of the input motion.

CHARACTERIZATION OF INPUT MOTIONS

In the subsequent sections, an attempt is made to characterize input motions in terms of frequency content, intensity and duration by examining each parameter individually. Alternative measures of frequency content and intensity are considered. Particular attention is placed on the relation of each measure to dynamic inelastic response.

By setting the duration of the input motion for most analyses at 10 seconds, using Housner's "spectrum intensity"(13) as a measure of intensity and noting certain trends in velocity response spectra, a basis is laid for the selection of acceleration records for use in dynamic analysis.

Duration Of Input Motion

Most strong-motion accelerograms recorded on firm alluvial soil contain a 5 to 15 second phase of relatively constant or stationary high-intensity oscillations with dominant frequencies between 2 and 5 cycles per second. Deterministic dynamic studies by Bogdanoff(14) have shown that structures subjected to a number of these ground motions experience their peak relative displacements during this short intense phase.

Penzien and Liu(15), on the basis of the nonstationary response of linear systems to stationary "white noise", suggest that for typically damped (5-10% of critical) linear systems with fundamental periods up to 2 seconds, a 10-second duration of excitation gives ample time for structures to reach their steady state conditions. They also noted that increasing the duration of excitation beyond 20 seconds has a relatively small effect of the probability distribution of peak response.

In a study of critical excitations for the design of earthquake-resistant structures, Drenick(16) also observed that damage to a structure is most likely to occur during the first 5 to 10 seconds of strong ground motion. For nonlinear structures, Clough and Benuska(17) have shown that the only significant effect of an increase in the duration of high-intensity base excitation is on the cumulative plastic rotations in critically stressed members.

The major effect of duration of the input motion (assuming no change in intensity) is thus on the magnitude of the cumulative deformations, the maximum response values remaining largely unaffected. In view of these observations, it was decided to use 10 seconds of base excitation for most analyses.

The need to limit the duration of input motion to a reasonable interval of the more intense phase of a record was also influenced by the significant computer cost involved in dynamic inelastic analysis. This is particularly true for the frame-wall and coupled wall systems planned for consideration during the latter part of this investigation.

An examination of recorded accelerograms(11) indicates that analyses using 20 seconds of strong ground motion should provide reasonably conservative estimates of cumulative deformation requirements. Vanmarcke and Lai(18) recently completed a study of the strong-motion duration of 140 horizontal components of earthquakes representing a broad range of magnitudes, epicentral distance, and site conditions. The study indicates about a 90% likelihood (mean = 9.27 sec., standard deviation = 8.76 sec.) that the strong-motion duration will be 20 seconds or less. The strong-motion duration was defined in this study as the interval over which the ground motion intensity, as measured by the integral of the square of the acceleration over the interval, is distributed uniformly at constant average power or frequency content. A small number of 20-second analyses were carried out mainly to serve as basis for adjusting the calculated cumulative response quantities corresponding to 10-second input motions. This is discussed in detail in Ref. 8.

Frequency Characteristics Of Input Motion

A typical strong-motion accelerogram shows an extremely complex series of oscillations. Examples of earthquake accelerograms, the NS and EW component of the May 28, 1940, Imperial

Valley earthquake as recorded at El Centro, are shown in Fig. 1[8]. Any such record may be thought of as a superposition of simple, constant-amplitude sinusoidal waves, each with a different frequency, amplitude and phase. The importance of knowing the frequency characteristics of a given input motion lies in the phenomenon of resonance or quasiresonance. This occurs when the frequency of the exciting force or motion approaches the frequency of the structure. Near maximum response to earthquake excitation can be expected if the dominant frequency components of the exciting motion occur in the same frequency range as the dominant effective frequencies of a structure.

A convenient way of studying the frequency characteristics of an accelerogram is provided by the Fourier amplitude spectrum. Figure 2, from Ref. 19, shows the Fourier amplitude spectra for the NS and EW components of the 1940 El Centro record. This spectrum provides a frequency decomposition of the accelerogram, indicating the amplitude (in units of velocity as a measure of the energy content) of the component at a particular frequency.

Another commonly used measure of the frequency content of an accelerogram is the velocity response spectrum. This is a plot showing the variation of the maximum absolute value of the relative velocity of a linear single-degree-of-freedom (SDF) system with the undamped natural period (or frequency) when subjected to a particular input motion. Figure 3 (Ref. 20) shows the relative velocity response spectra for the NS and EW components of the 1940 El Centro record, for different values of the damping factor (specified as a fraction of the critical damping coefficient). Hudson has shown[21] that when the maximum response of a system occurs at the end of the record, the undamped relative velocity response spectrum has a form identical to that of the Fourier amplitude spectrum of the ground acceleration. Under other conditions, these two plots are roughly similar. As in the Fourier spectrum, the peaks in the velocity response spectrum reflect concentrations of the input energy at or near the corresponding frequencies. For damped systems, these peaks are reduced, the reduction being greater for the shorter period systems.

Although both Fourier amplitude and undamped velocity response spectra exhibit a jagged character, with peaks and troughs occurring at close intervals, it is usually possible to recognize a general trend in the overall shape of the curve. By noting the general shape of the spectrum in the frequency range of interest, a characterization of the input motion in terms of frequency content can be made.

Classification of Accelerograms

In this study, a viscous damping coefficient of 5% of critical for the first mode was used as the basic value for the dynamic analysis model. Accordingly, the 5% damped velocity response spectra corresponding to 10 seconds of each of 20 selected records were examined. Figures 4a and 4b show the velocity response spectra for the NS and EW component of the 1940 El Centro motion. These results are based on the initial 10 seconds of the record. The remaining spectra considered are shown in Appendix A. On the basis of this examination, two general categories were recognized (Fig. 5):

1. A "peaking" accelerogram with a spectrum exhibiting dominant frequencies over a well-defined period range. The NS component of the 1940 El Centro record is an example of this class.
2. A "broad-band" accelerogram that has a more or less flat spectrum over the period range of interest. The vertical component of the 1940 El Centro record falls into this category.

   A sub-class of the broad-band category is a record with a spectrum which increases with increasing period within the period range of interest. This may be referred to as an "ascending" accelerogram. The EW component of the 1940 El Centro record is typical of this type of record.

The procedure proposed above represents a rather crude method for classifying accelerograms in terms of frequency content and does not account for the variation of frequency content with time[22]. Nevertheless, it provides a sufficient basis for determining the potential severity of a given input motion in relation to a specific structure.

Frequency Content and Structural Response

For a linear structure in which the dynamic behavior is dominated by the fundamental mode, as is the case in most reinforced concrete multistory buildings with structural walls, a strong response can be expected when the fundamental period falls within the peaking range of the input motion, i.e., when the period range of the dominant components of the input motion are similar to those of the structure. A weaker response can be expected if the dominant period of the structure falls outside the peaking range.

For isolated walls where only nominal yielding occurs, or for highly redundant structures such as frames and frame-wall systems, where yielding in some elements may not significantly change the effective period of the structure consequently, the initial fundamental period may continue to provide a good indication of the dynamic properties of the structure even beyond first yield. For these cases, a peaking accelerogram with its spectrum peak centered about the initial fundamental period will likely produce more severe response when compared to a broad-band accelerogram of the same intensity (Fig. 5a).

The effective period of a yielding structure changes with the extent of inelastic action and the general state of deformation of the structure i.e., loading or unloading. Thus, different components of an input motion will exert varying influences on the behavior of the structure at different times. Since the general effect of yielding is to increase the period of vibration, the longer-period components in a record will tend to play a greater role as yielding progresses in the structure.

In a structure such as an isolated wall, where yielding at and near the base can produce a significant increase in the effective period of vibration, a peaking accelerogram with the spectrum peak centered about the initial fundamental period of the structure produces its maximum effect prior to yielding. After yielding, the effect of the dominant frequency components diminishes as the effective period of the structure moves beyond the peaking range. For such a structure, a broad-band accelerogram of the same intensity may produce a more severe response as indicated in Fig. 5b.

The above observations have been verified for the particular case of isolated structural walls. This is discussed under Parametric Studies in Ref. 23.

Inventory of Acceleration Records

To have available a set of accelerograms representative of the two classes described earlier for use as input in dynamic analysis, a number of records were chosen from a compilation of natural records[11]. This list was augmented by a selection of artificially generated accelerograms. The records were chosen to provide a set of peaking accelerograms with 5%-damped-velocity-response-spectra peaking ranges covering the period range from about 0.5 to 3.0 seconds, as well as some broad-band accelerograms. The set of peaking accelerograms and their respective peaking ranges are listed in Table 1. Since the isolated structural walls considered in the dynamic analysis have fundamental periods varying from 0.5 to 3.0 seconds, there will be several records with their dominant frequency components near each of the basic structure periods.

The peaking ranges in Table 1 were determined visually such that the width of each range corresponds to an ordinate about two-thirds the peak value. The peaking ranges for the undamped spectra corresponding to the full records and those for the 5%-damped spectra corresponding to the first 10 seconds of each record are given. In general, the peaks of the undamped spectra for the shorter 10-second segments of an accelerogram occur in the same period ranges as for the full records; however, the values are slightly lower. The period domain for peak ranges for the 5%-damped spectra differ slightly from those for the undamped case mainly because of greater attenuation of the response due to damping for the shorter-period structures.

The artificially generated accelerograms include six of the CalTech design earthquake accelerograms (A-1, A-2, B-1, B-2, C-1 and C-2) generated by Jennings, Housner and Tsai[24]; five records generated using the program PSEQGN (denoted here as P-1 through P-5), developed by Ruiz and Penzien[25]; and six records generated using the program SIMQKE, developed by Gasparini[26]. The CalTech accelerograms A, B, and C were designed to simulate ground motions of varying intensity and duration corresponding to earthquakes of specific magnitude and epicentral distance. For instance, the A accelerograms are designed to represent ground motions close to the causative fault of a magnitude 8.5 (Richter scale) earthquake. The accelerograms P-1 through P-5 were generated to match, on the average, the spectrum, duration and peak acceleration of the NS component of the 1940 El Centro record.

Accelerograms generated using the program SIMQKE, denoted by S-1 through S-6, are designed to match a target response spectrum while retaining the general duration and envelope shape of typical strong-motion records. The target spectrum used for these records was essentially a flat, broad-band spectrum over the period range from 0.3 to 3.0 seconds. This spectrum is similar in shape to the design response spectra proposed by Newmark, Blume and Kapur[27].

To illustrate anticipated use of the assembled inventory, the selected accelerograms are classified according to whether they can be considered as "peaking" or "broad-band" with respect to a particular basic structure fundamental period. For this purpose, structures with initial fundamental periods of 0.8, 1.4, 2.0 and 2.4 seconds are assumed.

As a guide to the choice of input motions that may be used to excite a particular structure, Table 2 was prepared. Where they apply, two types of entries are shown under each period corresponding to a given accelerogram. An "A" is entered under a given period if the corresponding velocity response spectrum exhibits a narrow peak at or near the period of interest. A "B" indicates that the velocity response spectrum shows a relatively high plateau extending from the period of interest to at least one second longer.

Intensity Of Input Motions

The best parameter to use as a characteristic measure of the amplitude of the acceleration pulses within the period range of interest has not been clearly established. A commonly accepted measure of intensity is important if accelerograms are to be categorized according to intensity. Some investigators[28,29] have chosen to normalize accelerograms on the basis of the peak acceleration, velocity or displacement occurring within the portion of the record considered. Others have chosen to normalize input accelerograms in terms of the "spectrum intensity"[10]. This is the area under the relative velocity spectrum curve, between bounding values of the period range of interest. Others[30] have proposed using the integral of the square of the acceleration over the duration of the motion as a measure of intensity. Still others have used the root-mean-square (rms) acceleration, defined as,

$$\ddot{x}_{rms} = \left[\frac{1}{t} \int_0^t \ddot{x}^2 \, dt \right]^{1/2} \qquad (1)$$

Figure 6 shows the evolutionary rms acceleration plot for the first 20 seconds of the NS component of the 1940 El Centro record.

If the intensity measure is to reflect the variation of acceleration amplitude over the period range of interest, it must have the character of an average. By this criterion, the peak acceleration is a poor measure. The spectrum intensity, taken over the period range of interest and for a reasonable damping value, should yield a more representative measure of intensity.

On the basis of a study of the statistical properties of a number of strong-motion records, Liu[31] concluded that the stationary rms acceleration provides a good measure of earthquake intensity. He further showed that, for the earthquakes he considered, there exists a close correlation between the stationary rms acceleration and Housner's spectrum intensity.

The spectrum intensity and rms acceleration were calculated for the twenty horizontal components of the record listed in Table 1. The results are shown plotted in Fig.7, where the ordinate is the peak rms acceleration during the first 10 seconds of each record. The abscissa is the corresponding spectrum intensity (SI) defined between 0.1 and 3.0 seconds, for 5% damping and a 10 second duration. A linear relationship between the two quantitites is suggested, viz.,

$$\ddot{x}_{rms} = (0.51 \pm 0.12)\ SI \qquad (2)$$

On the basis of the above correlation, it appears that spectrum intensity is a satisfactory measure of the intensity of an earthquake.

<u>Spectrum Intensity Versus Ductility of SDF Systems</u>

To further investigate the appropriateness of the spectrum intensity as a measure of the intensity of an accelerogram, a study of the nonlinear response of single-degree-of-freedom (SDF) systems was undertaken. The system considered is characterized by a bilinear stable hysteretic force-displacement relationship. The object here was to determine if a correlation could be established between ductility requirement and spectrum intensity. In SDF systems, the ductility ratio is defined as the ratio of the maximum relative displacement to the displacement corresponding to first yield. For a given earthquake, the ductility ratio serves as a good index of damage in structures or, for a particular structure, it provides an indication of the potential destructiveness of an earthquake.

For this study, the first 10 seconds of nine sample records were considered and normalized in terms of spectrum intensity. Spectrum intensities equal to 0.75, 1.0 and 1.5 times the spectrum intensity of the initial 10 seconds of the NS component of the 1940 El Centro record at 5% damping were used. The yield displacement, Δ_y, of the structures considered were calculated from the relation,

$$\Delta_y = \frac{0.03gK}{\pi^2} T^{5/3} \tag{3}$$

Equation (3) is based on the 1973 Uniform Building Code[32] provision governing design base shear with an earthquake zone factor, Z = 1.0 and

$$C = \frac{0.05}{\sqrt[3]{T}} \tag{4}$$

In Eqs. (3) and (4), g is the acceleration due to gravity, K is the horizontal force factor as given in Reference 32; T is the fundamental period of the structure; and C is the base shear coefficient appearing in the expression for the design base shear: V = ZKCW. In this expression, W is the dead weight of the structure.

In deriving Eq. (3), a value of K = 0.80 was used and the yield force was assumed to be twice the design base shear. A yield stiffness ratio, $r_y = 0.05$ (i.e., the ratio of the slope of the post-yield branch to the initial slope of the force-deformation curve) and a viscous damping coefficient, = 0.05, were assumed.

Ductility ratios corresponding to SDF systems having different initial periods when subjected to different base motions were determined for the three intensities of each of nine sample records.

Figures 8a and 8b show the displacement response spectra and the velocity response spectra, respectively, corresponding to different intensities of the E-W component of the 1940 El

Centro record. In both figures, the scale factor "f" is the ratio of the spectrum intensity of the input motion used to the reference spectrum intensity. The figures indicate that for the bilinear stable hysteretic systems considered, both maximum displacements and velocities generally increase with an increase in the intensity of the input motion and the severity of the yielding. The curves corresponding to f = 1.0 in Fig. 8a show that maximum displacements for linear and bilinear systems are more or less the same over a broad period range, an observation also made by earlier investigators. Similar behavior was observed by Veletsos[33] in a study using a slightly different normalization scheme.

Figure 9 shows the variation of ductility ratio with period for the same acceleration record. Similar results were obtained by Clough and Johnston[34] using unscaled accelerograms and the same yield displacement-period relation, for K = 0.67.

The mean ductility ratio and the mean-ductility-ratioplus-one- (unbiased) standard-deviation are shown plotted against period in Fig. 10, for each intensity value of the nine-record sample. For any given period, both mean and standard deviation increase with increasing intensity.

Figures 11a and 11b show the variation of mean ductility with spectrum intensity for two specific initial periods. For simple, stable, hysteretic systems subjected to base motions normalized in terms of spectrum intensity, the mean ductility ratio correlates reasonably well with the spectrum intensity.

Based on these observations, it was decided to use the spectrum intensity as the characteristic measure of the intensity of an accelerogram. Where several acceleration records are to be considered as input in a parametric study, and intensity is not the parameter investigated, each accelerogram is normalized using a reference spectrum intensity.

In Refs. 8 and 23, intensity is normalized by scaling the ordinates of an acceleration record so that the spectrum intensity for 10 seconds of the record, at 5% of the critical damping, matches a specified proportion of the reference spectrum intensity corresponding to the NS component of the 1940 El Centro record. Factors of 0.75, 1.0 and 1.5 have been used. The factor 1.5 is generally thought to represent the magnitude of the motion from the largest earthquake reasonably expected in California[35]. Using the scaling procedure proposed by Guzman and Jennings[36], this scale factor corresponds roughly to the motion expected from a shallow focus 8.5-magnitude earthquake at an epicentral distance of about 8 to 10 miles.

SUMMARY

The major parameters characterizing strong-motion accelerograms - duration, frequency content and intensity - are investigated in an effort to minimize the number of input motions that need to be considered in establishing "critical" structural response to earthquakes.

Based on an examination of a large number of recorded strong-motion accelerograms, it is suggested that a 20-second duration of strong ground motion is sufficient to determine design requirements for most structures. It is also suggested that for calculating maximum response, the duration of input motions may be limited to 10 seconds of the most intense motion. The major effect of a longer earthquake duration is on cumulative deformation while the maximum response quantities remain largely unaffected. Thus, most analyses need not exceed 10 seconds. Cumulative deformation demands corresponding to the longer-duration motions can be readily estimated from the results of a few 20-second analyses.

The 5%-damped relative velocity response spectrum is adopted as a basis for defining the frequency characteristics of accelerograms. Accelerograms are classified into two general categories, depending on the shape of the associated velocity response spectrum. "Peaking" accelerograms have velocity spectra exhibiting dominant frequencies over a well-defined period range. The spectra of "broad-band" accelerograms, on the other hand, remain more or less flat over the period range of interest. It is pointed out that where significant yielding can be expected in a structure, with attendant increase in the effective period of vibration, an input motion with a broad-band velocity spectrum is likely to produce more severe deformations than a peaking accelerogram of the same intensity and duration. For cases where only nominal yielding is expected, peaking type accelerograms tend to produce more severe deformations.

A list of accelerograms representative of both types is assembled for use as input in dynamic structural analysis. It

should be possible to choose from this set a small number of accelerograms having the frequency content to critically excite a particular structure.

A comparison of the 5%-damped spectrum intensity (period range: 0.10 -3.0 sec.) with the corresponding evolutionary root-mean-square acceleration indicates that the spectrum intensity provides a reasonably good measure of the intensity of an accelerogram. A similar conclusion is supported by a comparison between the 5%-damped spectrum intensity and the ductility demand in bilinear stable single-degree-of-freedom systems. It is suggested that where several acceleration records are to be used as input in dynamic analysis, and particularly in parametric studies where intensity is not the parameter investigated, the acceleration ordinates should be adjusted to yield the same spectrum intensity.

REFERENCES

1. Applied Technology Council, Recommended Comprehensive Seismic Design Provisions for Buildings, Final Review Draft, ATC-3-05, Applied Technology Council, Palo Alto, California, January 7, 1977.

2. Appendix A, Building Code Requirements for Reinforced Concrete (ACI 318-77), American Concrete Institute, P.O. Box 19150, Redford Station, Detroit, Michigan 48219.

3. The Behavior of Reinforced Concrete Buildings Subjected to the Chilean Earthquakes of May 1960," Advanced Engineering Bulletin No. 6, Portland Cement Association, Skokie, Illinois, 1963.

4. Fintel, M., "Quake Lesson from Managua: Revise Concrete Building Design?" Civil Engineering, ASCE, August 1973, pp. 60-63.

5. Anonymous, "Managua, If Rebuilt on Same Site, Could Survive Temblor," Engineering News Record, December 6, 1973, p. 16.

6. Derecho, A.T., Fugelso, L.E. and Fintel, M., "Structural Walls in Earthquake-Resistant Buildings - Analytical Investigations, Dynamic Analysis of Isolated Structural Walls - INPUT MOTIONS," Final Report to the National Science Foundation RANN, under Grant No. ENV74-14766 Portland Cement Association, January 1978.

7. Derecho, A.T., Ghosh, S.K., Iqbal, M., Freskakis, G.N., Fugelso, L.E., and Fintel, M., "Structural Walls in Earthquake-Resistant Buildings - Analytical Investigation, Dynamic Analysis of Isolated Structural Walls (Part A: Input Motions and Part B: Parametric Studies)," Report to the National Science Foundation RANN, under Grant No. GI-43880, Portland Cement Association, October 1976.

8. Derecho, A.T., Iqbal, M., Ghosh, S.K., Fintel, M., and Corley, W.G., "Structural Walls in Earthquake-Resistant Buildings - Analytical Investigation, Dynamic Analysis of Isolated Structural Walls - DEVELOPMENT OF DESIGN PROCEDURE - DESIGN FORCE LEVELS," Final Report to the National Science Foundation, RANN, under Grant No. ENV74-14766, Portland Cement Association, March 1978.

9. Oesterle, R.G., Fiorato, A.E., Johal, L.S., Carpenter, J.E., Russell, H.G. and Corley, W.G., "EarthquakeResistant Structural Walls - Tests of Isolated Walls," Report to the National Science Foundation, Portland Cement Association, Nov. 1976, 44 pp. (Appendix A, 38 pp.; Appendix B, 233 pp.)

10. Derecho, A.T., Iqbal, M., Ghosh, S.K., M. Fintel, and Corley, W.G., "Structural Walls in Earthquake-Resistant Buildings - Analytical Investigation, Dynamic Analysis of Isolated Structural Walls - REPRESENTATIVE LOADING HISTORY," Final Report to the National Science Foundation, RANN, under Grant No. ENV74-14766, Portland Cement Association, March 1978.

11. Analysis of Strong Motion Earthquake Accelerograms, Vol. II, Corrected Accelerograms Parts A, B, C, Report EERL 72-79, California Institute of Technology, Earthquake Engineering Research Laboratory, 1972, 1973, 1974.

12. Guzman, R., Crouse, C.B., and Jennings, P.C., "Determination of Design Earthquakes for Nuclear Power Plants," Technical Report No. 50-T22, Fugro, Inc., 1975.

13. Housner, G.W., "Behavior of Structures During Earthquakes," Journal of the Engineering Mech. Division, ASCE, Paper No. 2220, October 1959.

14. Bogdanoff, J.L., "Comments on Seismic Accelerograms and Response Spectra," (Preliminary Report) Joint U.S.-Japanese Seminar in Applied Stochastics, NSF-JSPS, Tokyo, May 1966.

15. Penzien, J., and Liu, S-C., "Nondeterministic Analysis of Nonlinear Structures Subjected to Earthquake Excitation," Proc. 4th World Conference on Earthquake Engineering, Vol. I, Chile, January 1969.

16. Drenick, R.F., "Prediction of Earthquake Resistance of Structures," Polytechnic Institute of Brooklyn, New York, Final Report to the National Science Founation on Grant GK 14550, May 1972, 128 pp.

17. Clough, R.W. and Benuska, K.L., "FHA Study of Seismic Design Criteria for High-Rise Buildings," Report HUD TS-3, Federal Housing Administration, Washington, D.C., August 1964.

18. Vanmarcke, E.H. and Lai, S.P., "Strong-Motion Duration of Earthquakes," Publication No. R77-16, Order No. 569, Department of Civil Engineering, Massachusetts Institute of Technology, 32 pp., July 1977.

19. Analysis of Strong Motion Earthquake Accelerograms, Vol. IV, Fourier Spectra, Part A, Report EERL 71-81, California Institute of Technology, Earthquake Engineering Research Laboratory, 1972.

20. Analysis of Strong Motion Earthquake Accelerograms, Vol. III - Response Spectra, Part A - Accelerograms IIA001 through IIA020, Report EERL 72-80, California Institute of Technology, Earthquake Engineering Research Laboratory, August 1972.

21. Hudson, D.E., "Some Problems in the Application of Response Spectrum Techniques to Strong-Motion Earthquake Analysis," Bulletin of the Seismological Society of America, Vol. 52, No. 2, April 1962.

22. Saragoni, G.R. and Hart, G.C., "Time Variation of Ground Motion Frequency Content: Characterization and Relevance," Proceedings of the Fifth World Conference on Earthquake Engineering, Rome, 1973, Session 4A, Paper No. 156.

23. Derecho, A.T., Ghosh, S.K., Iqbal, M., Freskakis, G.N. and Fintel, M., "Structural Walls in Earthquake-Resistant Buildings - Analytical Investigation, Dynamic Analysis of Isolated Structural Walls - PARAMETRIC STUDIES," Final Report to the National Science Foundation, RANN, under Grant No. ENV74-14766, Portland Cement Association, March 1978.

24. Jennings, P.C., Housner, G.W. and Tsai, N.C., "Simulated Earthquake Motions for Design Purposes," Proc. 4th World Conference on Earthquake Engineering, Vol. I, Chile, 1969.

25. Ruiz, P. and Penzien, J., "Probabilistic Study of the Behavior of Structures During Earthquakes," Earthquake Engineering Research Center Report No. EERC 69-3, University of California, Berkeley, March 1969.

26. Gasparini, D., "SIMQKE: A Program for Artificial Motion Generation," Internal Study Report No. 3, Dept. of Civil Engineering, Massachusetts Institute of Technology, January 1975.

27. Newmark, N.M., Blume, J.A. and Kapur, K.K., "Seismic Design Spectra for Nuclear Power Plants," Proc. ASCE Journal of the Power Division, P02, 1973, pp. 287-303.

28. Frank, R. and Gasparini, D., "Evaluation of Seismic Safety of Buildings: Progress Report on Statistical Studies of Response of MDOF Systems to Real and Artifical Ground Motions," Internal Study Report No. 4, Dept. of Civil Engineering, Massachusetts Institute of Technology, January 1975.

29. Goel, S.C. and Berg, G.V., "Inelastic Earthquake Response of Tall Steel Frames," Journal of the Structural Division, ASCE, Paper No. 6061, August 1968.

30. Arias, A., "A Measure of Earthquake Intensity," in Seismic Design for Nuclear Power Plants, R.J. Hansen, Editor, pp. 438-483, The MIT Press, Cambridge, Massachusetts, 1970.

31. Liu, S-C, "Statistical Analysis and Stochastic Simulation of Ground-Motion Data," The Bell System Technical Journal, 47, pp. 2273-2248, 1968.

32. International Conference of Building Officials, Uniform Building Code, 1963 Edition, 5360 South Workman Mill Road, Whittier, California 90601.

33. Veletsos, A.S., "Maximum Deformations of Certain Nonlinear Systems," Structural Research at Rice, Report No. 1, Dept. of Civil Engineering, Rice University.

34. Clough, R.S. and Johnston, S.B., "Effect of Stiffness Degradation on Earthquake Ductility Requirements," Proc., Japan Earthquake Engineering Symposium, 1966.

35. Derecho, A.T. and Fintel, M., "Earthquake Resistant Structures," Chapter 12 in Concrete Engineering Handbook, ed. by M. Fintel, Van Nostrand Reinhold, New York, 1974

36. Guzman, R. and Jennings, P.C., "Determination of Earthquake Design Spectra for Nuclear Power Plants," Technical Report No. 51-T22, Fugro, Inc., 1975.

ACKNOWLEDGMENTS

This investigation was carried out in the Engineering Services Department of the Portland Cement Association, Skokie, Illinois. Mr. Mark Fintel, then Director of Engineering Services, now Director of Advanced Engineering Services, served as overall Project Director of the combined analytical and experimental program. The help extended by Dr. S. K. Ghosh, Senior Structural Engineer, Advanced Engineering Services, and Dr. W. G. Corley, Director, Engineering Development Department, in reviewing the draft of this report is gratefully acknowledged.

The project was sponsored, in major part, by the National Science Foundation, RANN Program, through Grant No. ENV74-14766.

TABLES AND FIGURES

Table 1 - Period Ranges of Peak Velocity Response for Selected Accelerograms

Earthquake Description	Cal Tech No.#	Component	Period Range of Dominant Velocity Response (sec.)	
			Undamped Spectrum for Entire Record	5% Damped Spectrum for Initial 10 sec. of Record
Imperial Valley, May 18, 1940	A001	S00E	0.4 - 1.2	0.4 - 1.2
El Centro Site, Imperial Valley Irrigation District	A001	S90W	0.3 - 1.6 (1.9 - 2.3)	1.9 - 3.0
	A001	Vert	0.1 - 3.0	0.1 - 3.0 (0.6 - 1.0)
Kern County, July 21, 1952	A002	S00E	0.9 - 2.1	2.4 - 3.0
Pasadena - Cal Tech Athenaeum*	A002	S90W	0.7 - 1.0 (1.4 - 2.5)	0.7 - 1.1
	A002	Vert	0.8 - 1.3	0.6 - 1.2
Kern County, July 21, 1952	A004	N21E	0.3 - 0.9	0.4 - 1.6
Taft Lincoln School Tunnel	A004	S69E	0.3 - 0.9	0.4 - 3.0
	A004	Vert	0.2 - 0.8	
Kern County, July 21, 1952 Hollywood Storage P. E. Lot	A007	S00N	0.9 - 1.4	0.8 - 1.2
Eureka, December 21, 1954 Eureka Federal Building	A008	N11W	1.0 - 1.6 (2.1 - 2.7)	1.0 - 1.6
Eureka, December 21, 1954	A009	N44E	1.4 - 1.7	1.3 - 2.4
Ferndale City Hall	A009	N46W	1.3 - 1.7	0.9 - 1.7
	A009	Vert	1.8 - 2.2	1.4 - 2.0

#See Reference (1). *Second 10 seconds of record.

Table 1 (cont'd.) - Period Ranges of Peak Velocity Response for Selected Accelerograms

Earthquake Description	Cal Tech No.	Component	Period Range of Dominant Velocity Response (sec.)	
			Undamped Spectrum for Entire Record	5% Damped Spectrum for Initial 10 sec. of Record
El Almo, Baja, California	A011	S00W	0.8 - 1.2	1.2 - 1.9
February 9, 1956	A011	S90W	0.9 - 1.5	1.0 - 1.3
El Centro, Imperial Valley	A011	Vert	1.0 - 2.0	0.4 - 2.4
Borrego Mountain, April 8, 1968	A019	S00W	1.5 - 2.5	1.5 - 2.4
El Centro, Imperial Valley	A019	S90W	1.3 - 1.6 (2.1 - 2.4)	1.9 - 3.0
Borrego Mountain, April 8, 1968	A020	S00W	1.3 - 2.2	1.1 - 3.0
San Diego Light and Power Bldg.	A020	S90W	1.2 - 2.2	0.9 - 2.2
Parkfield, June 27, 1966	B036	N50E	1.3 - 1.7	1.2 - 1.6
Cholame, Shandon Array No. 12	B036	N40W	1.4 - 2.1	1.6 - 2.4
	B036	Vert	2.3 - 3.0	2.4 - 3.0
San Fernando, February 9, 1971	C041	S16E	0.8 - 1.8	0.9 - 2.0
Pacoima Dam	C041	S74W	0.3 - 0.6	0.4 - 1.7
	C041	Vert	0.2 - 0.6 (1.6 - 2.5)	
San Fernando, February 9, 1971	C048	S00W	1.3 - 2.4	1.5 - 2.2
8544 Orion Blvd., 1st Floor	C048	S90W	2.5 - 3.0	1.5 - 2.0
	C048	Vert	2.2 - 2.9	

NOTE: ( ) denotes secondary peak.

Table 2 - Classification of Selected Accelerograms in Terms of the Shape of Their 5%-Damped Velocity Response Spectra (Duration = 10 sec.)

Accelerogram	Component	Type of Record @			
		Period (sec.)			
		0.8	1.4	2.0	2.4
Imperial Valley, 5-18-40	NS	A	-	B	-
El Centro	EW	-	B	B	B
	Vert	B	B	B	B
Kern County, 2-21-52	N21E	A	-	-	-
Taft Lincoln School Tunnel	S69E	B	B	B	-
San Fernando, 2-9-71	S16E	-	A	-	-
Pacoima Dam	S74W	-	B	-	-
San Fernando, 2-9-71	NS	-	-	A	-
8544 Orion Blvd.	EW	-	-	A	-
Kern County, 2-21-52	NS	A	-	-	-
Cal Tech Athenaeum	EW	A	-	-	-
	Vert	A	-	-	A
Eureka, 12-21-52	N11W	B	B	-	-
Eureka Federal Building					
Eureka, 12-21-52	N44E	-	B	-	-
Ferndale City Hall	N46W	B	A	-	-
	Vert	A	B	-	-
El Alamo, 2-9-56	NS	B	A	-	-
El Centro	Vert	-	B	-	-
Borrego Mt., 4-8-68	NS	-	-	B	B
El Centro	EW	-	-	B	B

@ A - "Peaking" relative to specified period value
B - "Broad band"

Table 2 (cont'd.) - Classification of Selected Accelerograms in Terms of the Shape of Their 5%-Damped Velocity Response Spectra (Duration = 10 sec.)

Accelerogram	Component	Type of Record			
		Period (sec.)			
		0.8	1.4	2.0	2.4
Borrego Mt., 4-8-68 San Diego L/P	EW	A	A	B	B
Kern County, 2-21-52 Hollywood Storage Building	NS	A	-	-	-
Parkfield, 5-27-66	N40W	B	B	B	B
Cholame, Shandon No. 12	N50E	-	A	-	-
Cal Tech-Artificial	A1	B	A	-	-
(Jennings, Housner, Tsai)	A2	B	B	A	-
	B1	B	-	-	B
	B2	B	A	-	-
	C1	B	B	-	-
	C2	B	B	-	-
PSEQGN-Artificial	P1	B	B	B	B
(Ruiz, Penzien)	P2	-	A	B	B
	P3	A	-	B	B
	P4	A	-	B	B
	P5	-	B	B	B
SIMQKE-Artificial	S1	B	B	B	B
(Gasparini)	S2	B	B	B	B
	S3	-	-	B	B
	S4	B	B	B	B
	S5	A	B	B	B

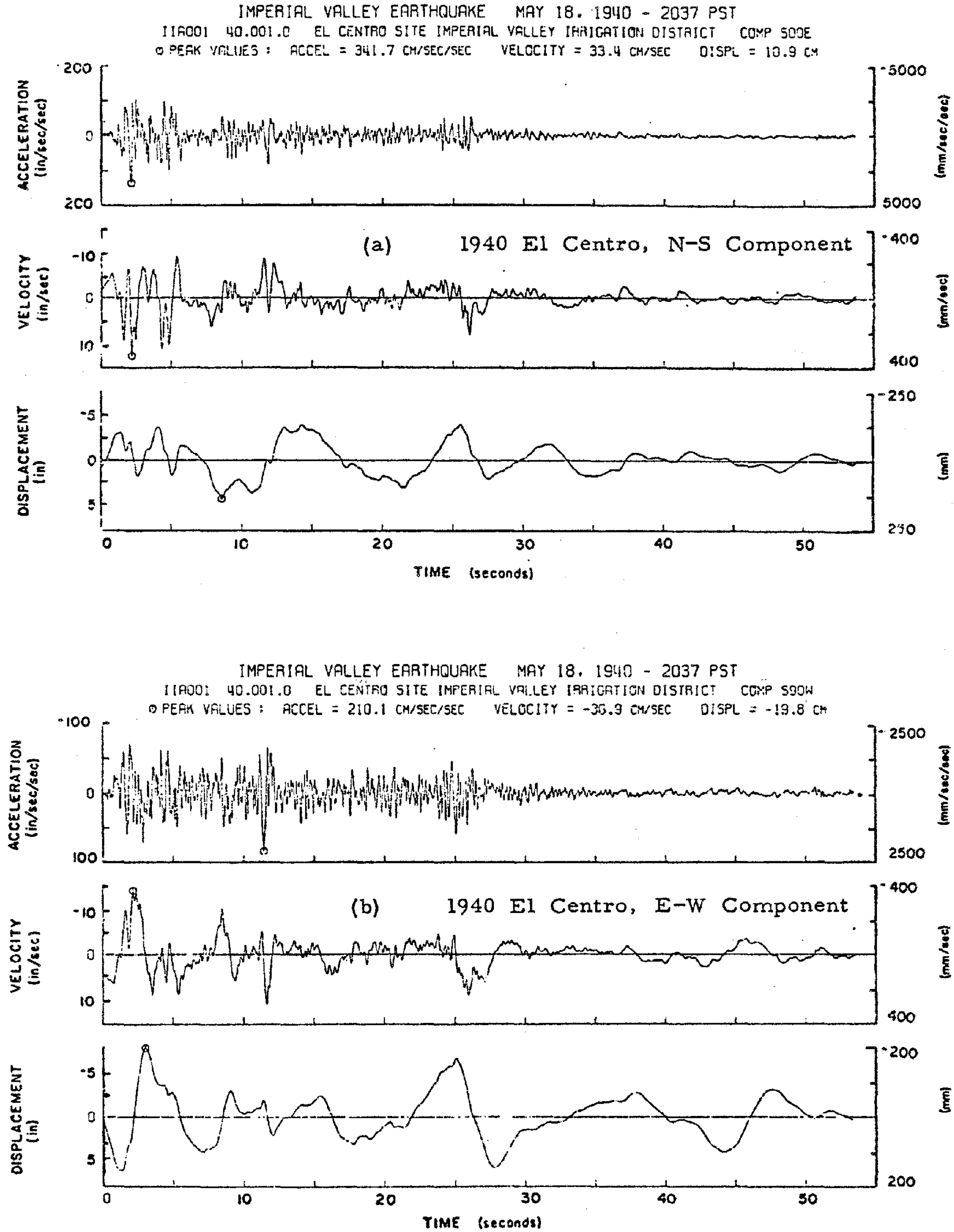

Fig. 1 Acceleration, Velocity and Displacement Histories 1940 El Centro record (from Ref. 11)

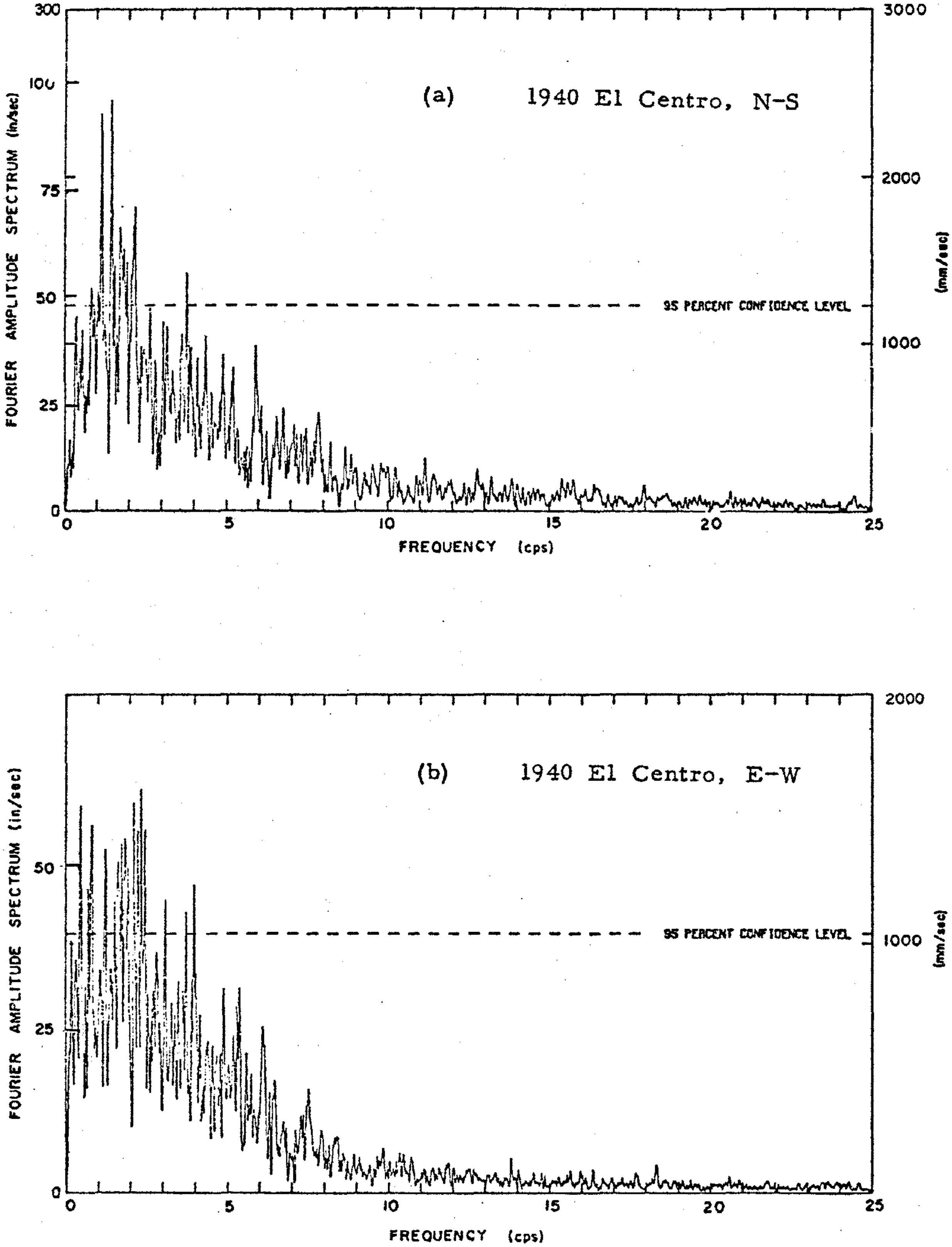

Fig. 2 Fourier Amplitude Spectrum - 1940 El Centro Record (from Ref. 19)

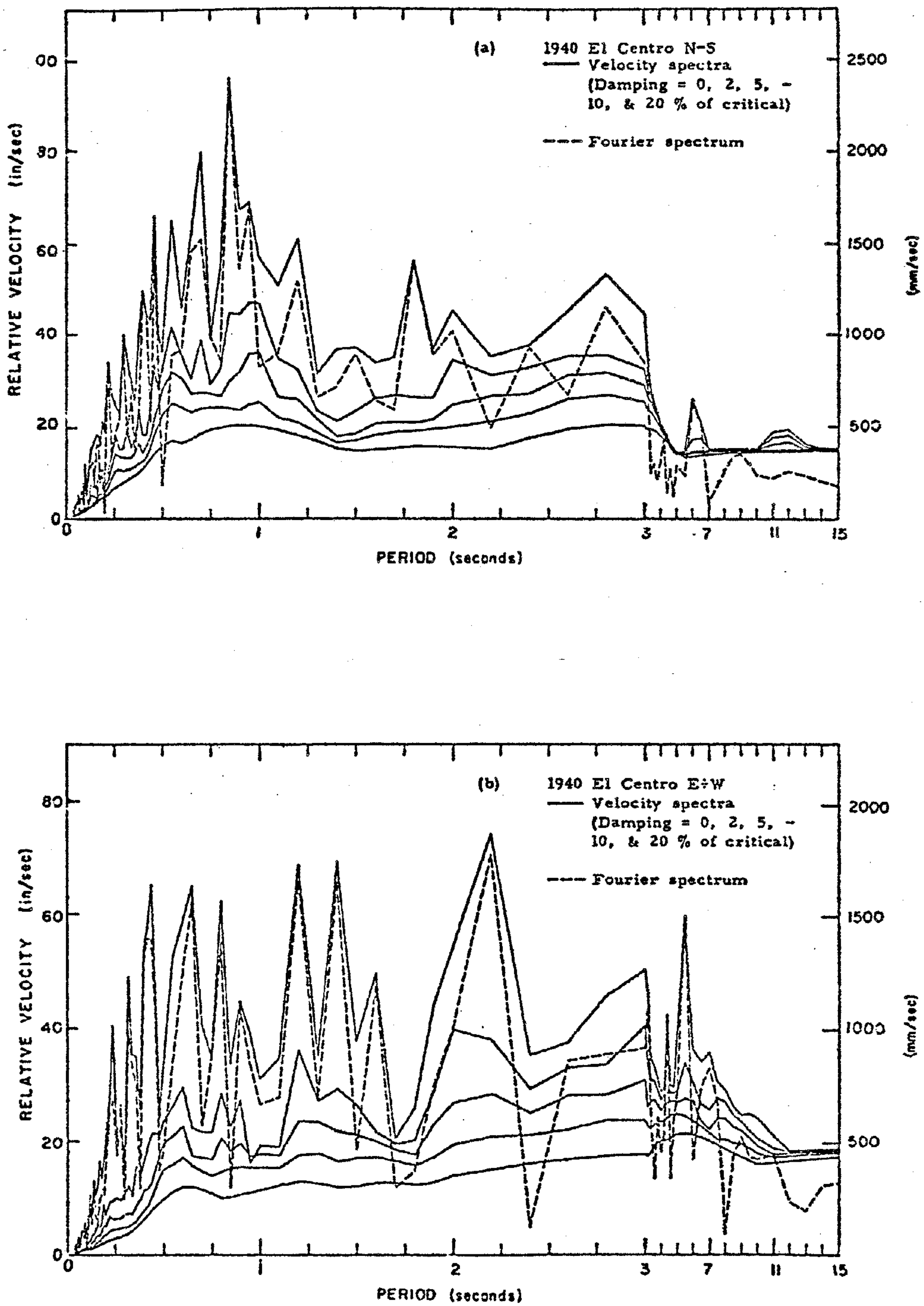

Fig. 3 Relative Velocity Response Spectra - 1940 El Centro Record (from Ref. 20)

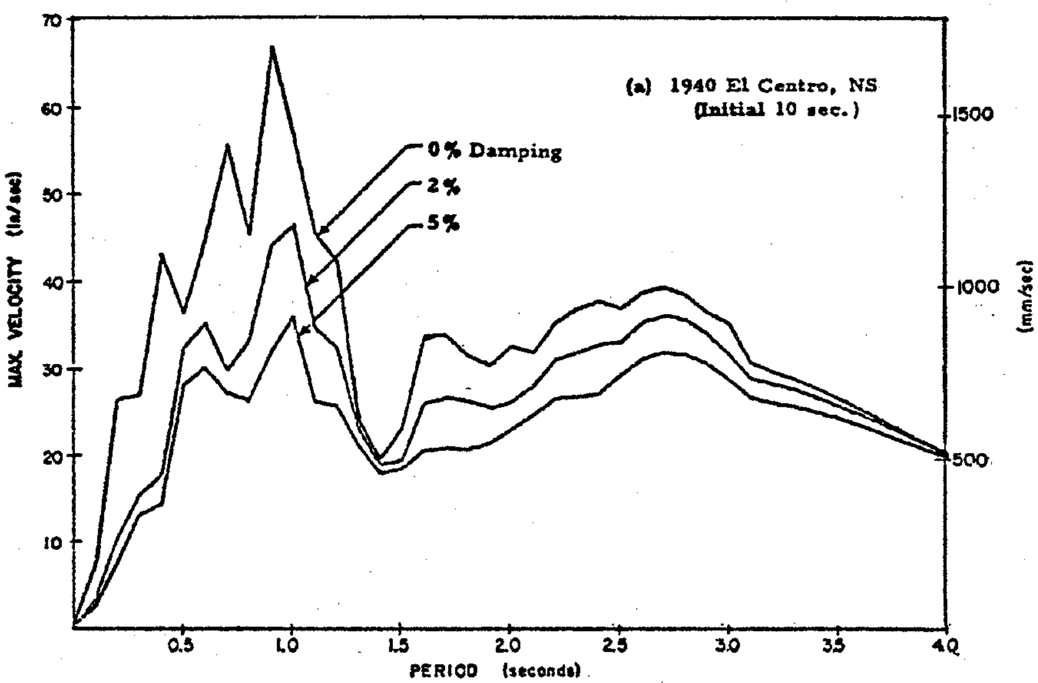

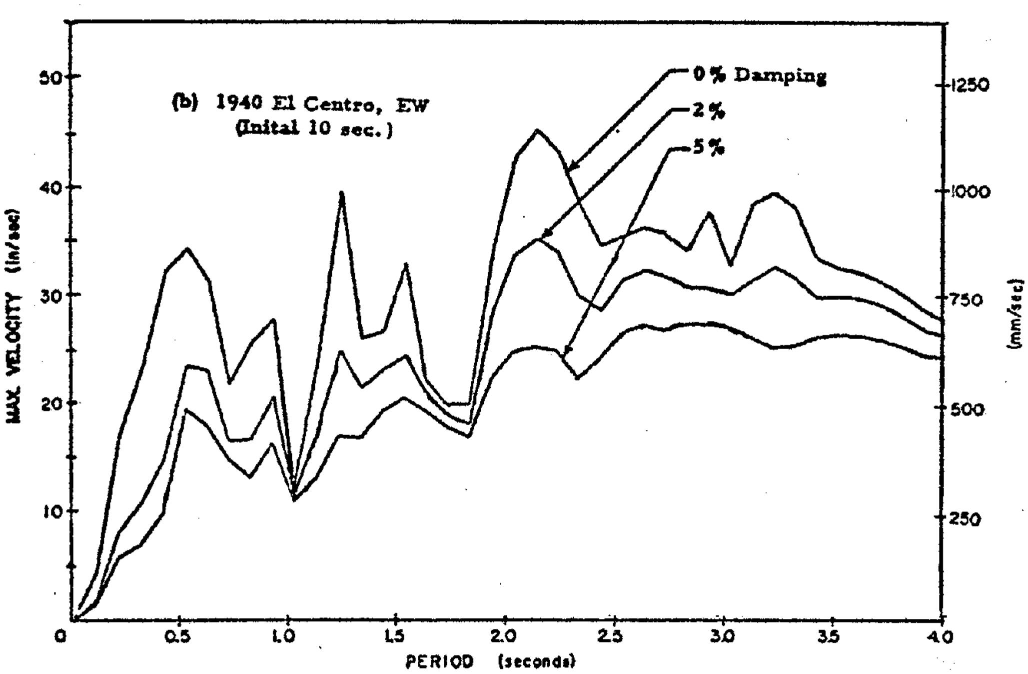

Fig. 4 Relative Velocity Response Spectra
1940 El Centro Record

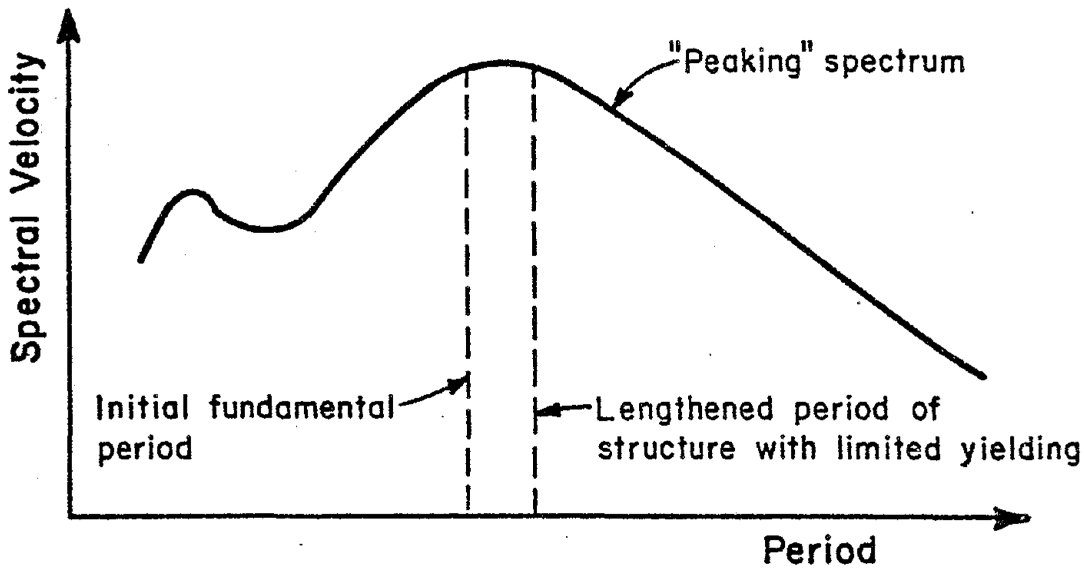

(a) Peaking Spectrum

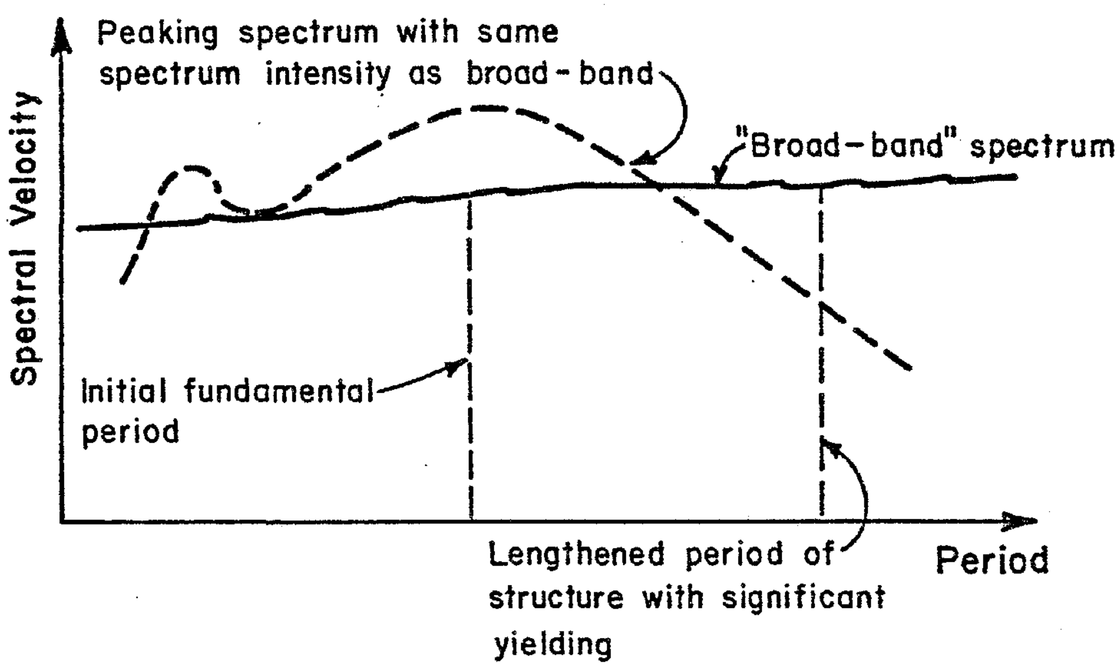

(b) Broad-band Spectrum

Fig. 5 Typical Basic Shapes of Damped Velocity Response Spectra

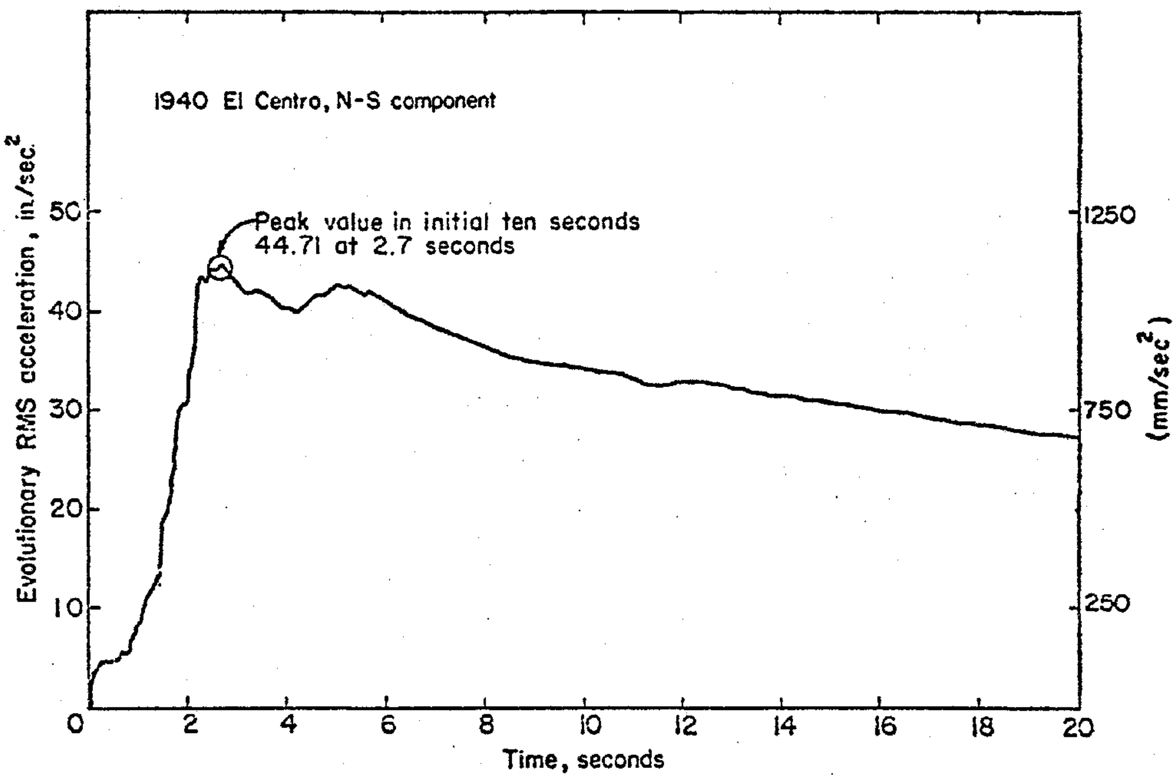

Fig. 6 Evolutionary RMS Acceleration versus Time

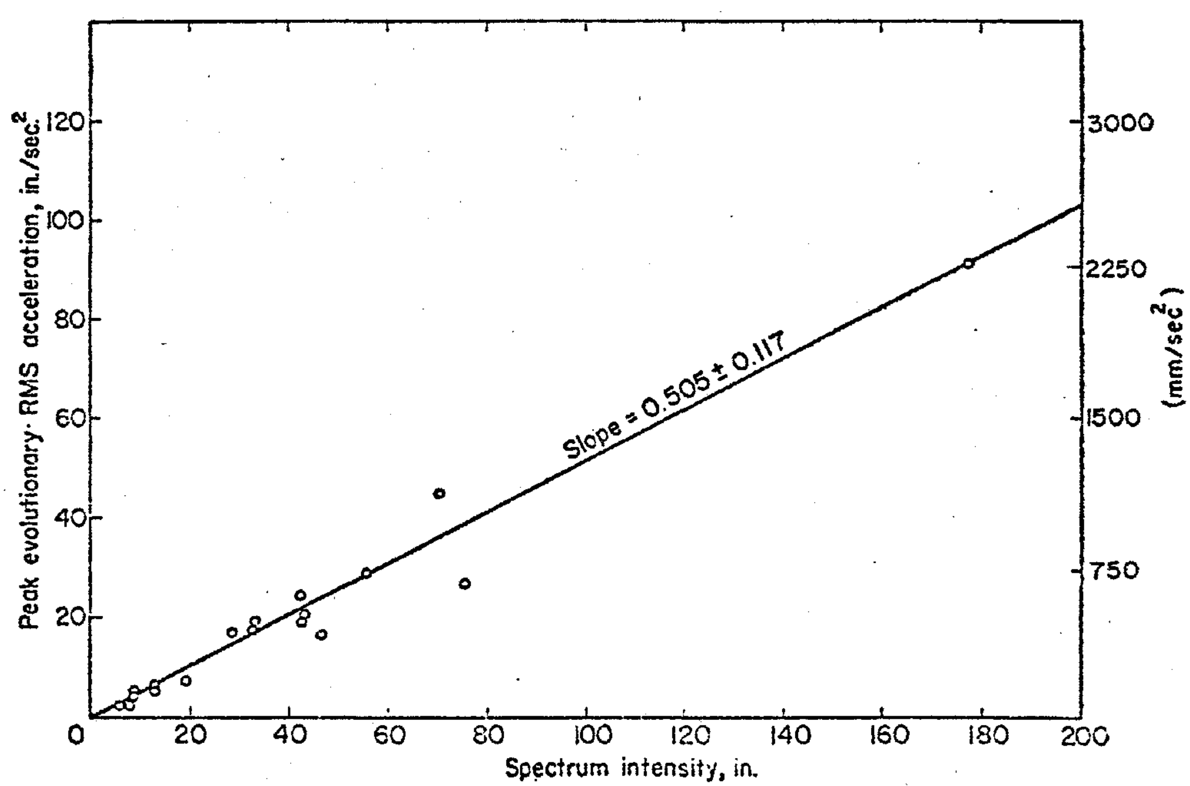

Fig. 7 Peak Evolutionary RMS Acceleration in First 10 Seconds vs. Spectrum Intensity for First 10 Seconds

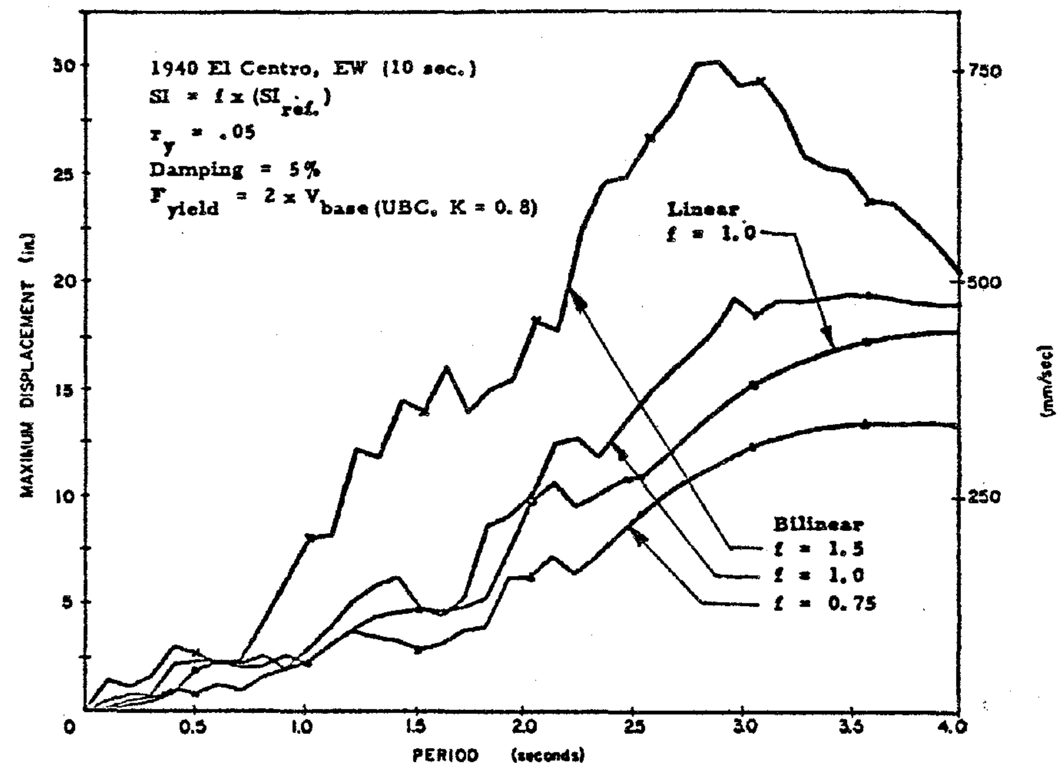

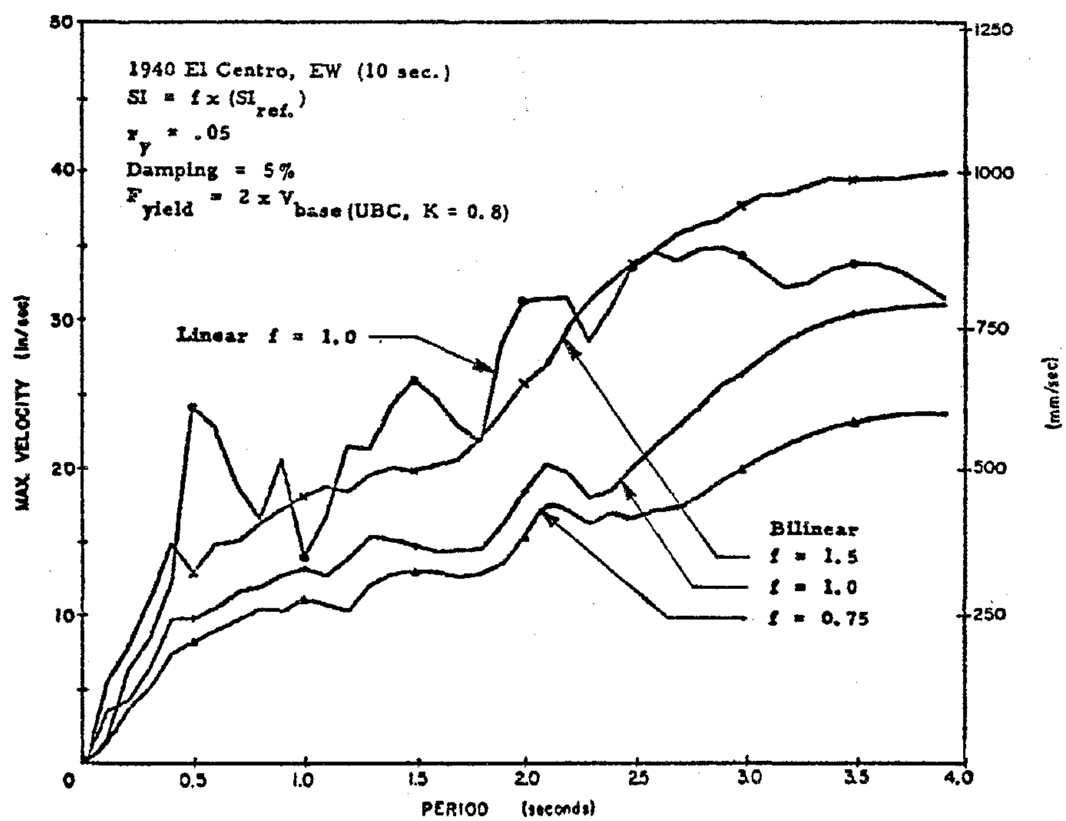

Fig. 8 Velocity Response Spectra for Linear and Bilinear Stable Hysteretic SDF Systems Subjected to Input Motions of Varying Intensity

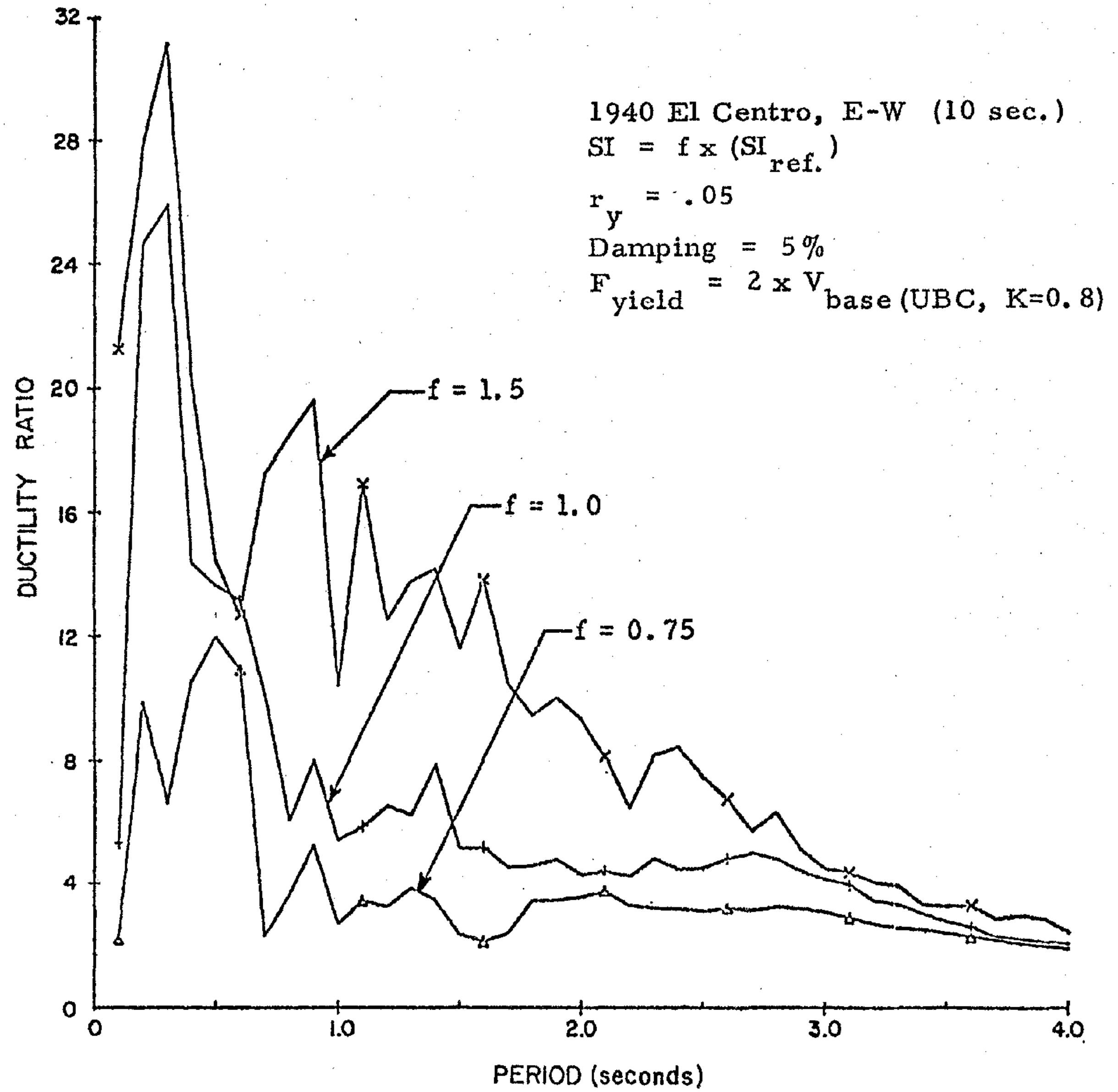

Fig. 9 Ductility Ratio versus Period for Bilinear Stable Hysteretic SDF Systems Subjected to Input Motions of Varying Intensity

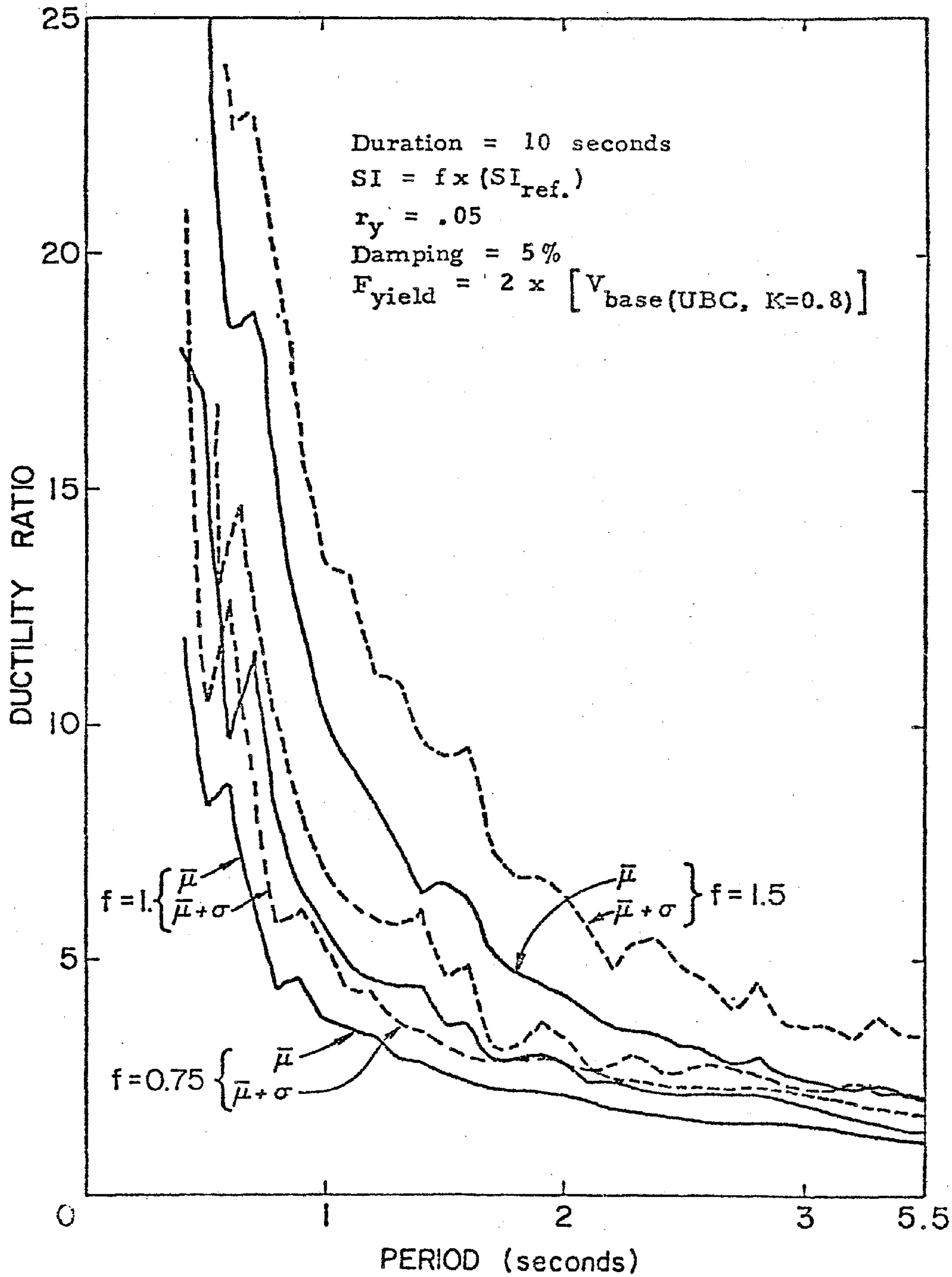

Fig. 10 Mean Ductility Ratio versus Period for Bilinear Stable SDF Systems

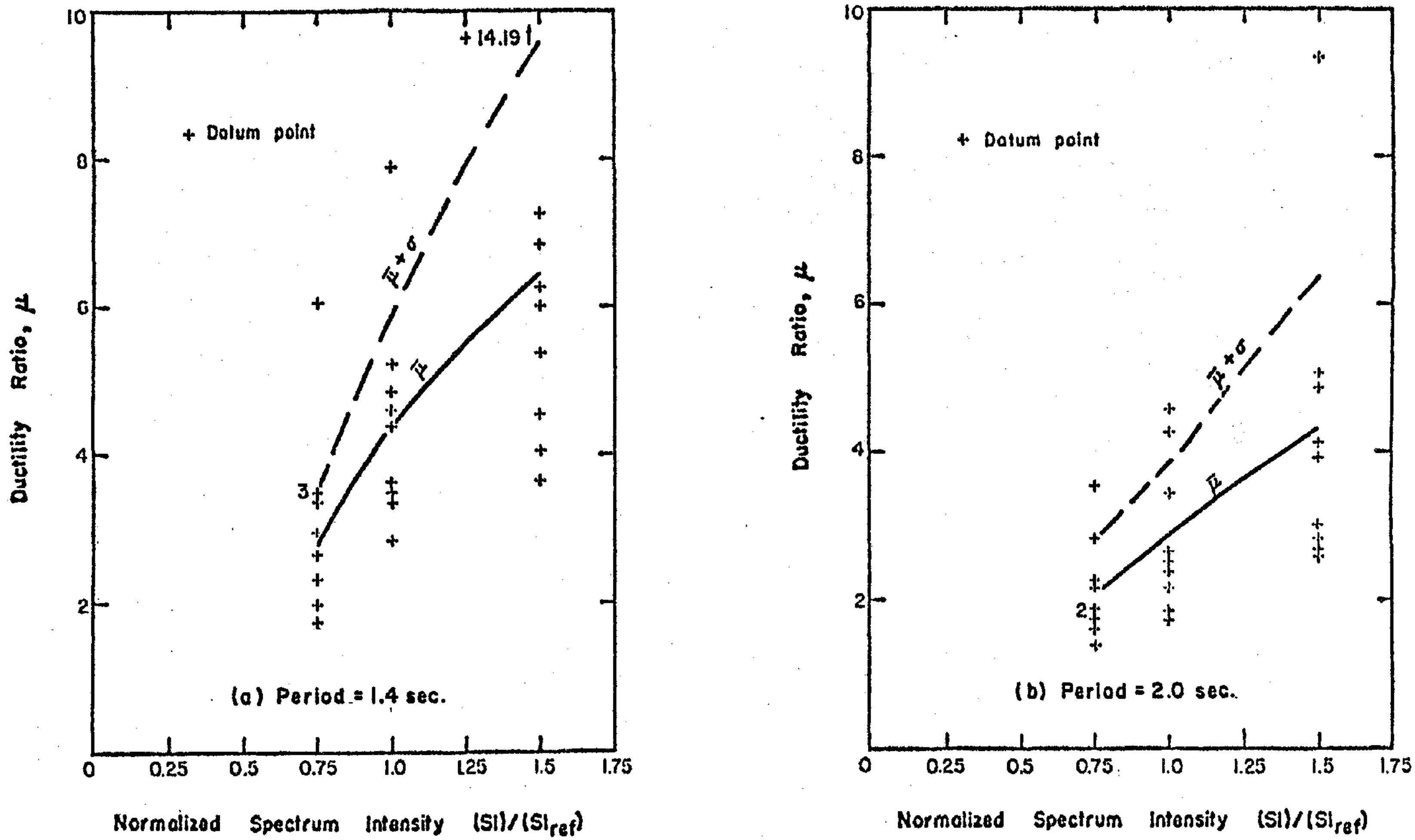

Fig. 11 Ductility Ratio versus Spectrum Intensity for Nine Input Motions - Bilinear Stable Hysteretic SDF Systems

APPENDIX A

Velocity Response Spectra for 10-Second Accelerograms

The velocity response spectra corresponding to the most intense portion of the natural and artificial accelerograms selected for this study are shown in Figures A-1 through A-42. Three values of damping, Vix., 0%, 2% and 5% of critical were evaluated. The spectrum intensities for these records, based on the period interval 0.1 to 3.0 seconds, are listed in Table A-1.

Table A1 - Spectrum Intensities for Selected Accelerograms Corresponding to Initial 10 Seconds of Record*

Accelerogram	Component	Spectrum Intensity (inches)		
		0% Damping	2% Damping	5% Damping
El Centro, 5-18-40	NS	106.26	83.39	70.15
	EW	87.89	68.57	55.97
	Vert	22.90	17.76	14.69
Kern County, 2-21-52	N21E	44.35	34.61	28.67
Taft Lincoln School Tunnel	S69E	49.60	40.38	33.35
San Fernando, 2-9-71	S74W	182.02	141.19	116.20
Pacoima Dam	S16E	244.85	207.78	177.25
San Fernando, 2-9-71	NS	60.34	50.54	42.87
Holiday Inn, Orion Blvd.	EW	48.41	39.55	32.67
Kern County, 7-21-52	NS	18.43	15.34	13.06
Cal Tech Athenaeum	EW	29.48	23.48	19.30
(2nd 10 seconds)	Vert	9.97	8.03	6.66
Eureka, 12-21-52	N11W	59.06	50.13	43.39
Eureka Federal Building				
El Alamo, 2-9-56	NS	12.90	10.32	8.39
El Centro	EW	18.09	14.97	12.61
	Vert	2.99	2.34	1.90
Eureka, 12-21-52	N44E	96.63	85.50	75.18
Ferndale City Hall	N46W	61.65	53.81	46.83
	Vert	16.36	14.28	12.46
Kern County, 7-21-52	NS	20.02	15.31	12.47
Hollywood Storage Building				

*except where noted.

Table A1 (cont'd.) - Spectrum Intensities for Selected Accelerograms Corresponding to Initial 10 Seconds of Record

Accelerogram	Component	Spectrum Intensity (inches)		
		0% Damping	2% Damping	5% Damping
Borrego Mt., 4-8-68	NS	53.59	48.24	42.33
El Centro	EW	10.91	9.68	8.64
Borrego Mt., 4-8-68	NS	9.64	8.82	7.93
San Diego L/P	EW	7.49	6.50	5.71
Parkfield, 6-27-66	N40W	12.62	9.76	8.02
Cholame, Shandon	N50E	12.83	10.32	8.44
Array No. 12	Vert	7.08	5.67	4.71
Cal Tech-Artificial	A1	137.03	114.01	94.79
(Jennings, Housner, Tsai)	A2	117.11	101.15	86.33
	B1	94.29	77.28	65.36
	B2	92.59	76.58	62.93
	C1	19.30	16.37	14.38
	C2	17.24	13.89	11.50
SIMQKE-Artificial	S1	104.86	79.18	63.46
(Gasparini)	S2	106.67	82.86	67.57
	S3	54.00	44.01	36.43
	S4	55.87	43.05	34.84
	S5	90.47	67.78	56.60
	S6	93.85	70.22	58.21
PSEQGN-Artificial	P1	64.82	49.55	39.82
(Ruiz, Penzien)	P2	109.40	86.53	70.84
	P3	105.21	82.98	66.57
	P4	131.77	108.49	91.01
	P5	214.27	181.49	152.81

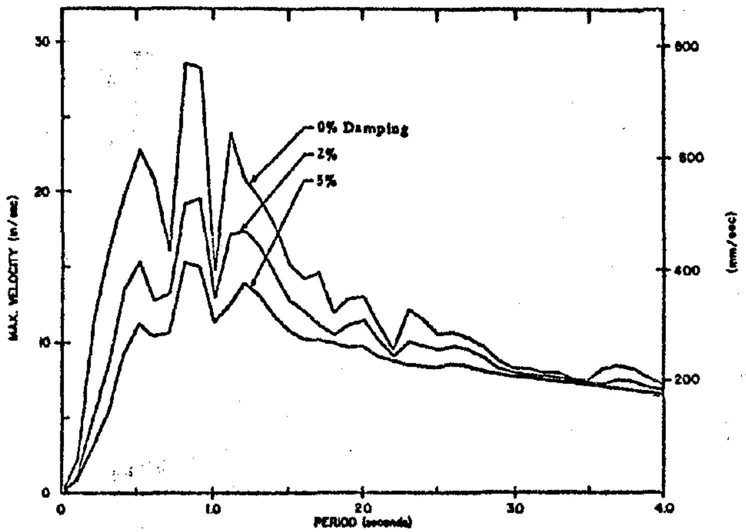

Fig. A1 Velocity Response Spectrum
Initial 10 Seconds, Kern County E/Q, 7-21-52
Taft Lincoln School Tunnel, N21E Component

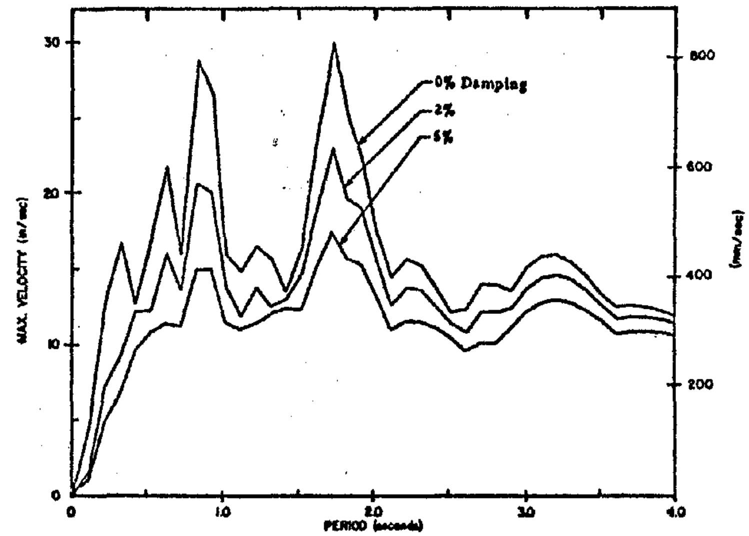

Fig. A2 Velocity Response Spectrum
Initial 10 Seconds, Kern County E/Q, 7-21-52
Taft Lincoln School Tunnel, S69E Component

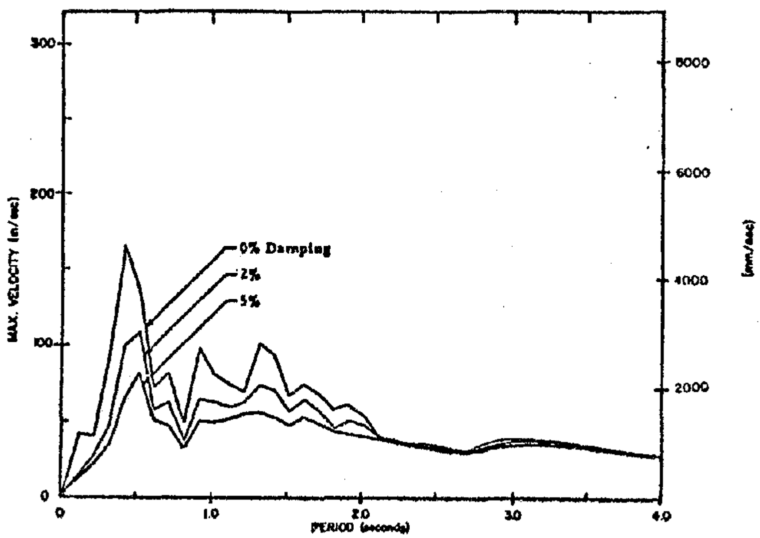

Fig. A3 Velocity Response Spectrum
Initial 10 Seconds, San Fernando E/Q, 2-9-71
Pacoima Dam, S74W Component

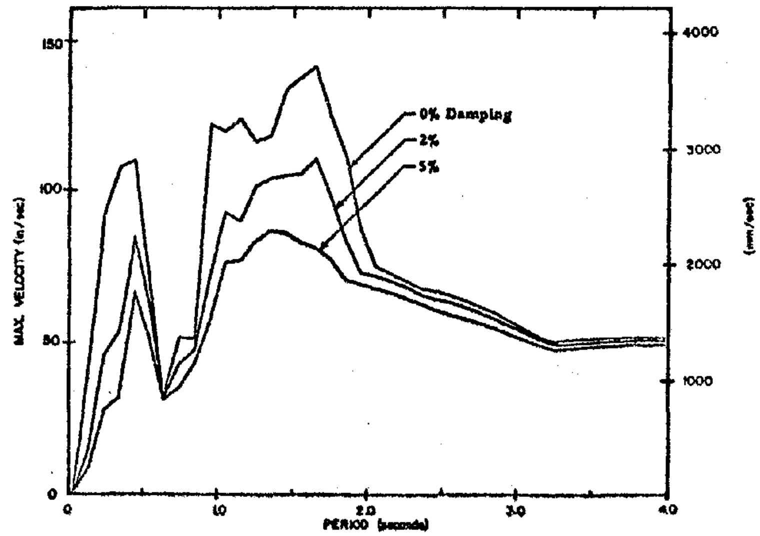

Fig. A4 Velocity Response Spectrum
Initial 10 Seconds, San Fernando E/Q, 2-9-71
Pacoima Dam, S16E Component

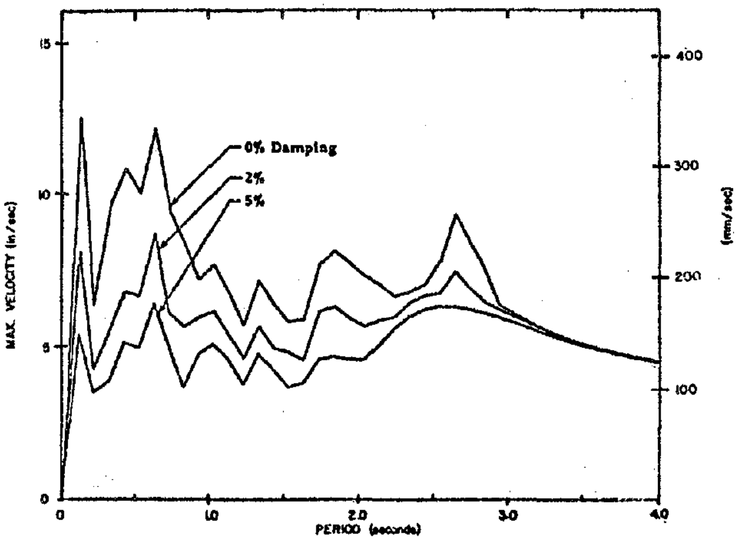

Fig. A5 Velocity Response Spectrum
Initial 10 Seconds, Imperial Valley E/Q, 5-18-40
El Centro, Vertical Component

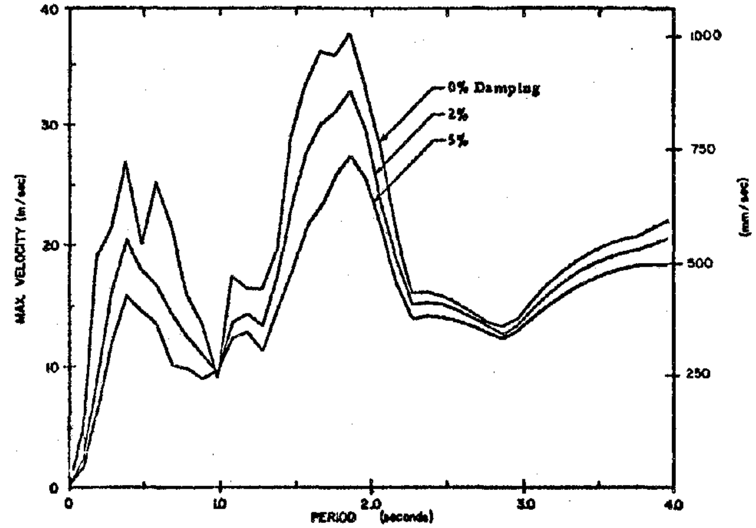

Fig. A6 Velocity Response Spectrum
Initial 10 Seconds, San Fernando E/Q, 2-9-71
8244 Orion Blvd., 1st Floor, NS Component

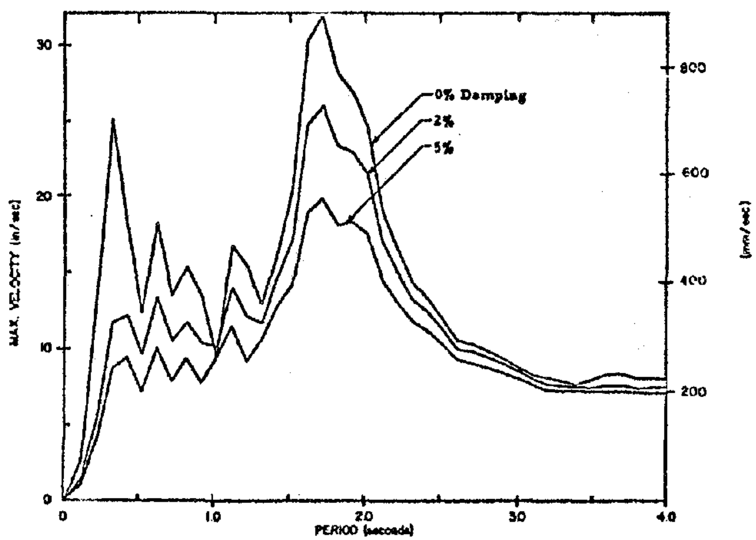

Fig. A7 Velocity Response Spectrum
Initial 10 Seconds, San Fernando E/Q, 2-9-71
8244 Orion Blvd., 1st Floor, EW Component

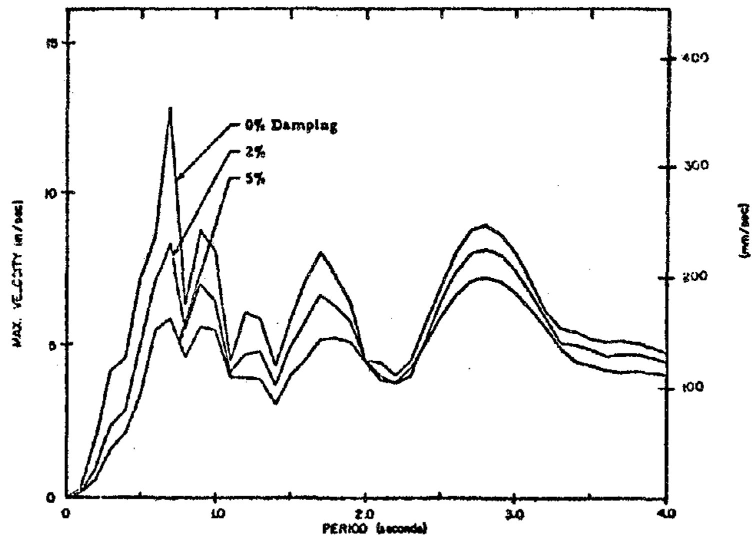

Fig. A8 Velocity Response Spectrum
Second 10 Seconds, Kern County E/Q, 7-21-52
Cal. Tech. Athenasum, NS Component

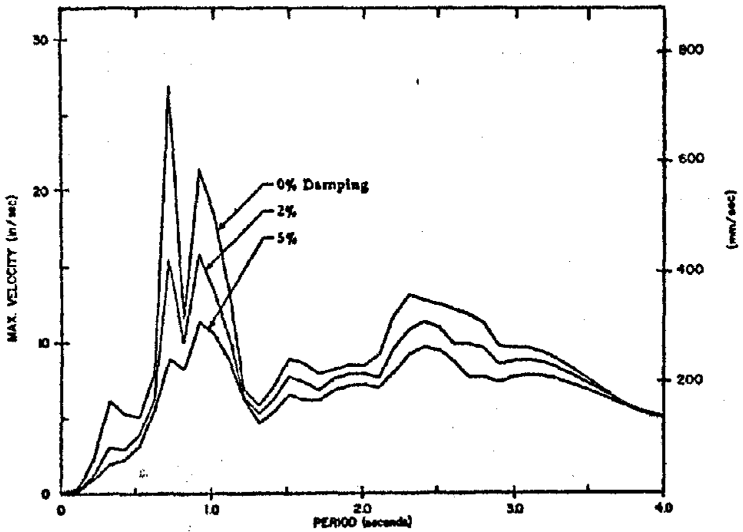

Fig. A9 Velocity Response Spectrum
Second 10 Seconds, Kern County E/Q 7-21-52
Cal. Tech. Athenasum, EW Component

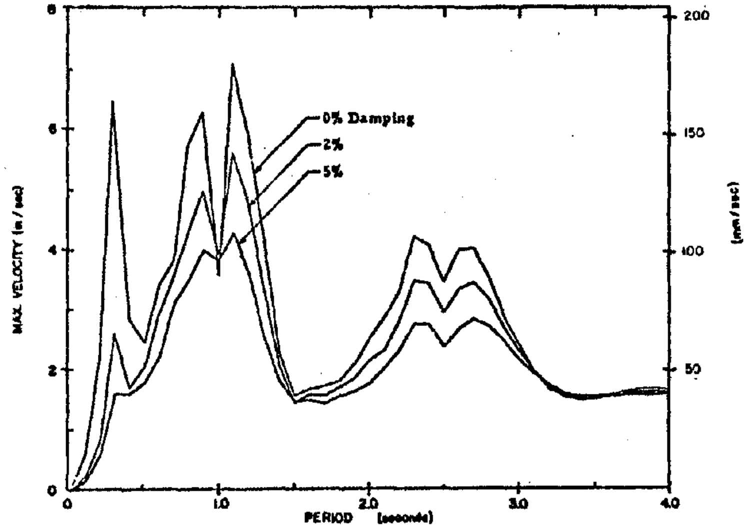

Fig. A10 Velocity Response Spectrum
Second 10 Seconds, Kern County E/Q, 7-21-52
Cal. Tech. Athenasum, Vertical Component

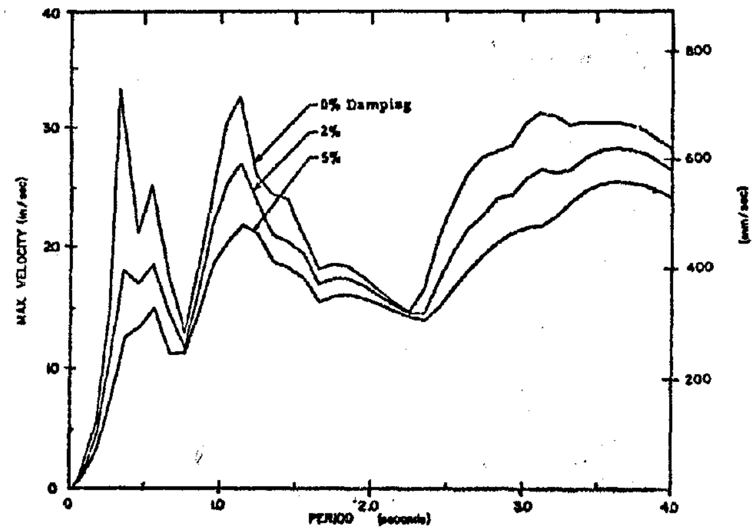

Fig. A11 Velocity Response Spectrum
Initial 10 Seconds, Eureka E/Q, 12-21-54
Eureka Federal Building, NHW Component

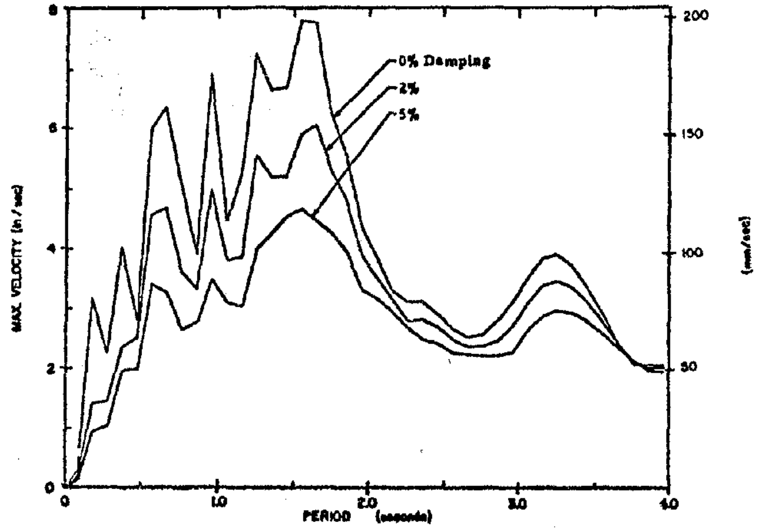

Fig. A12 Velocity Response Spectrum
Initial 10 Second, El Alamo E/Q, 2-9-56
El Centro, NS Component

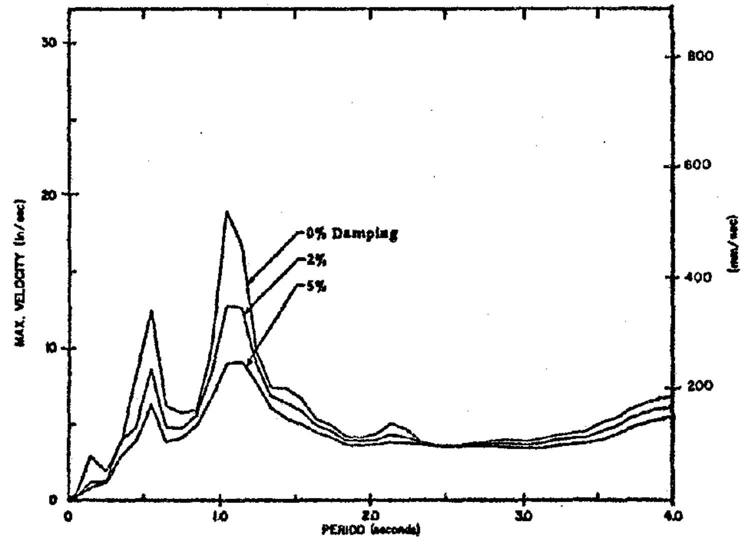

Fig. A13 Velocity Response Spectrum
Initial 10 Seconds, El Alamo E/Q, 2-9-56
El Centro, EW Component

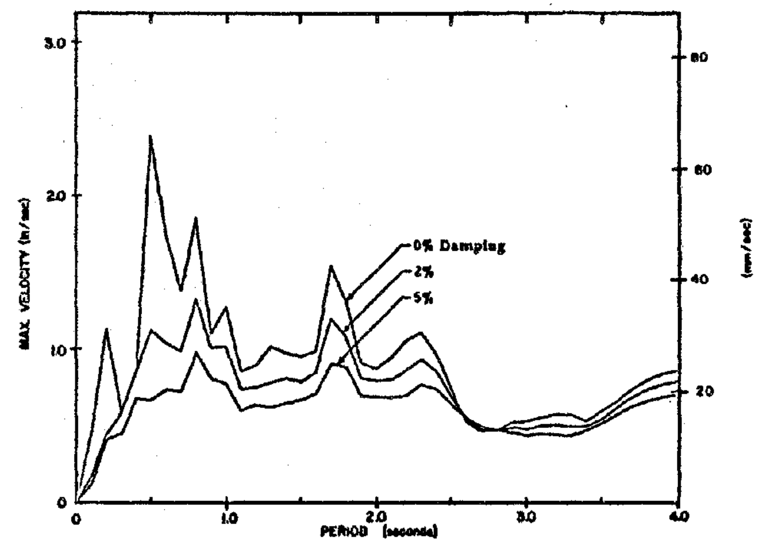

Fig. A14 Velocity Response Spectrum
Initial 10 Seconds, El Alamo E/Q, 2-9-56
El Centro, Vertical Component

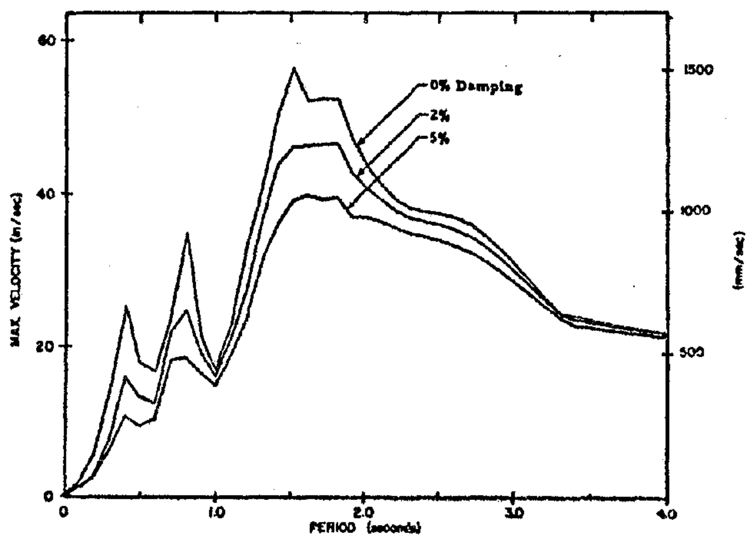

Fig. A15 Velocity Response Spectrum
Initial 10 Seconds, Eureka E/Q, 12-21-54
Ferndale City Hall, N44E Component

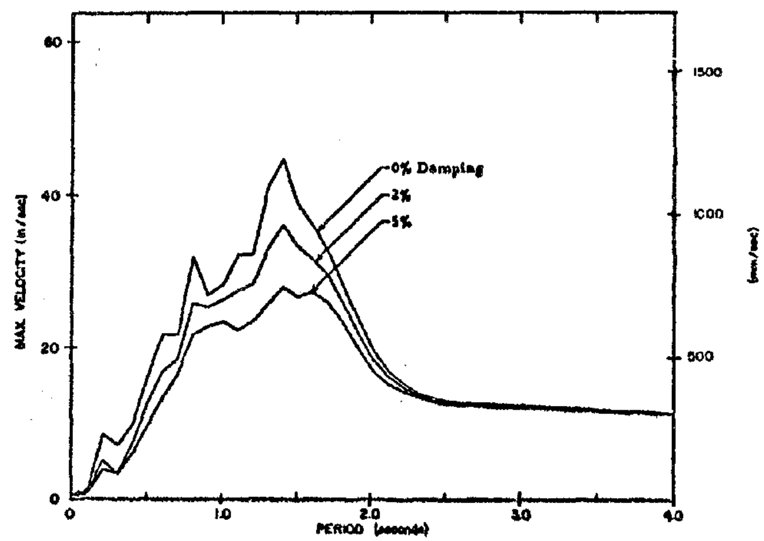

Fig. A16 Velocity Response Spectrum
Initial 10 Seconds, Eureka E/Q, 12-21-54
Ferndale City Hall, N46W Component

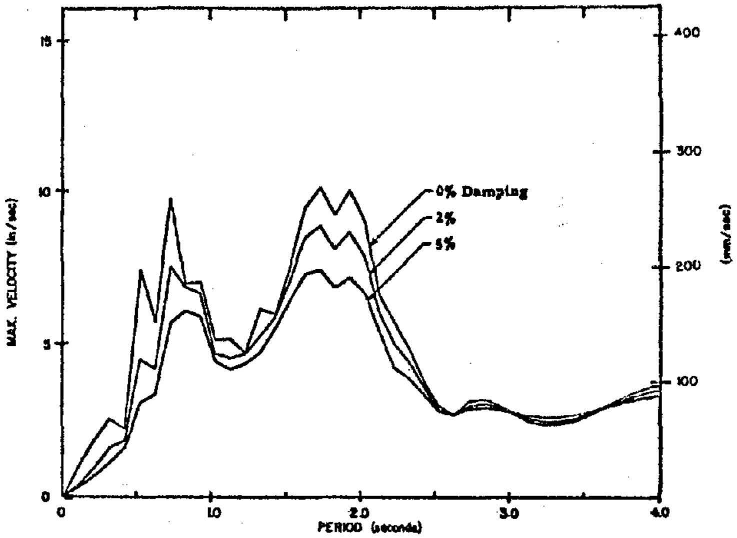

Fig. A17 Velocity Response Spectrum
Initial 10 Seconds, Eureka E/Q, 12-21-54
Ferndale City Hall, Vertical Component

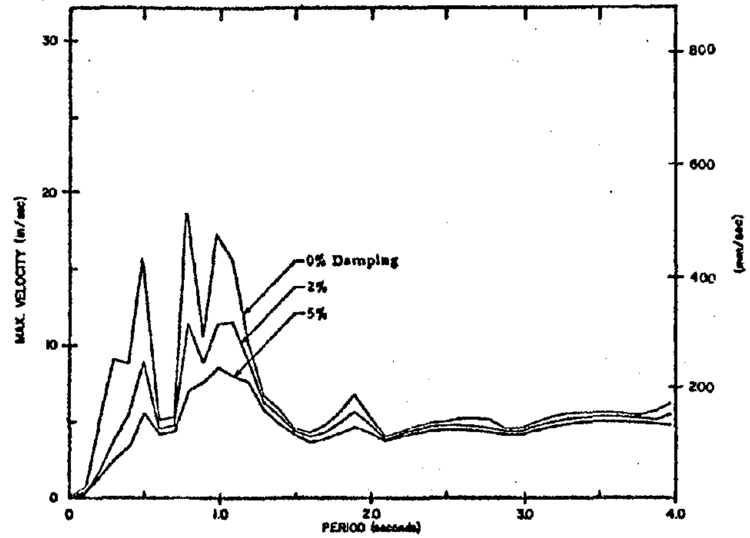

Fig. A18 Velocity Response Spectrum
Initial 10 Seconds, Kern County E/Q, 2-21-52
Hollywood Storage Building, P. E. Lot, NS Component

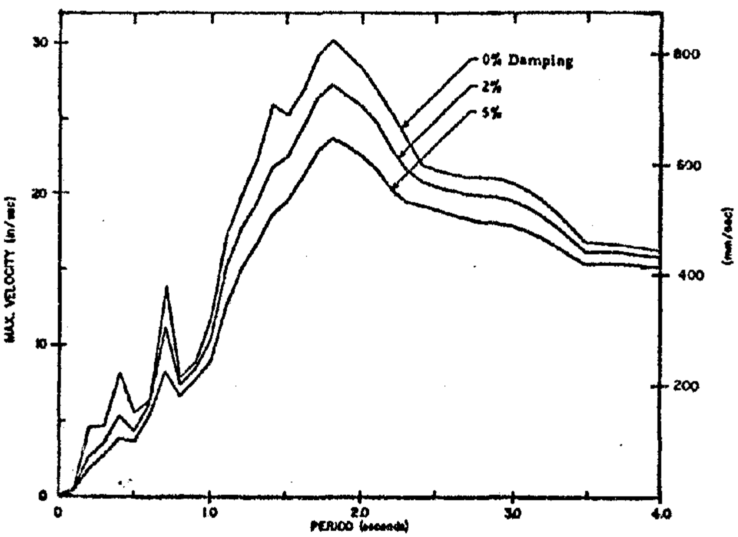

Fig. A19 Velocity Response Spectrum
Initial 10 Seconds, Borrego Mt. E/Q, 4-8-68
El Centro, NS Component

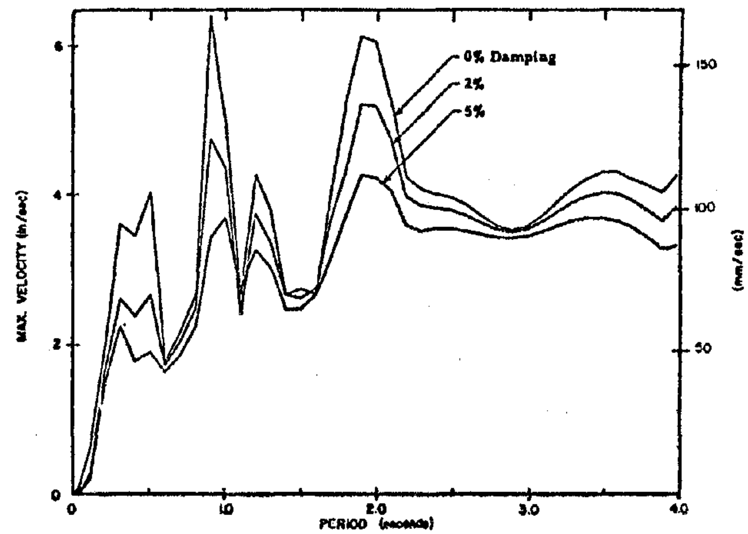

Fig. A20 Velocity Response Spectrum
Initial 10 Seconds, Borrego Mt. E/Q, 4-8-68
El Centro, EW Component

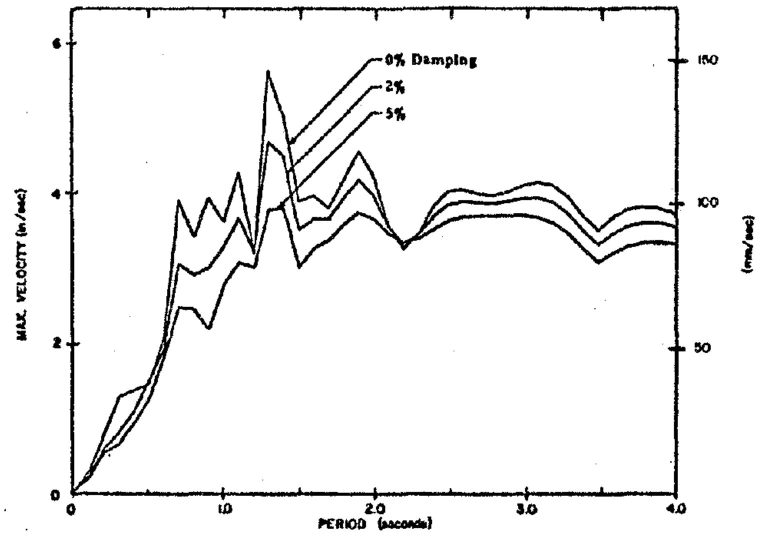

Fig. A21 Velocity Response Spectrum
Initial 10 Seconds Borrego Mt. E/Q. 4-8-68
San Diego Light and Power Building, NS Component

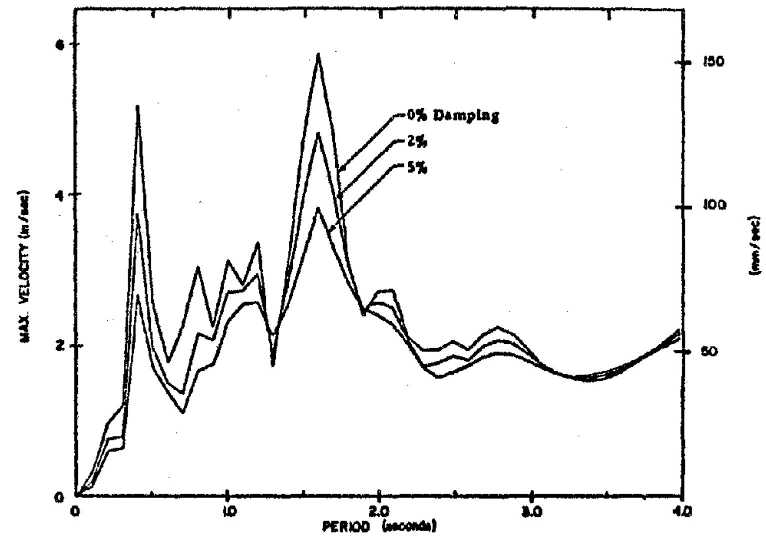

Fig. A22 Velocity Response Spectrum
Initial 10 Seconds, Borrego Mt. E/Q. 4-8-68
San Diego Light and Power Building, EW Component

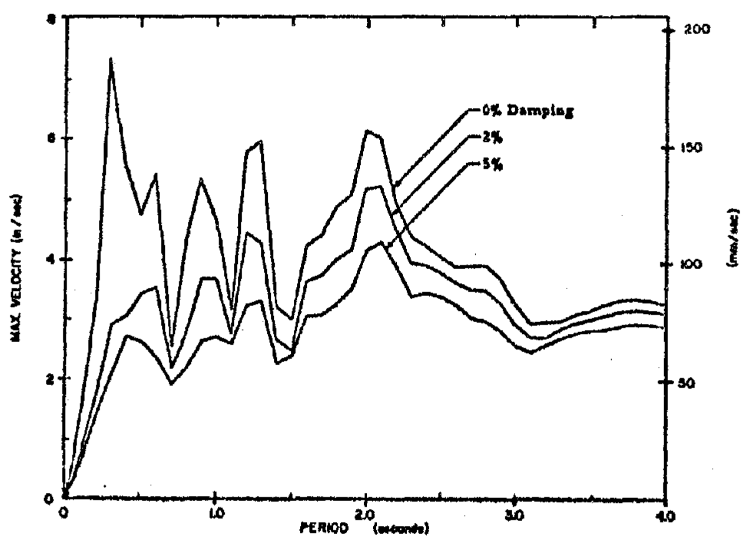

Fig. A23 Velocity Response Spectrum
Initial 10 Seconds, Parkfield E/Q. 6-27-66
Cholame-Shandon Array No. 12, N40W Component

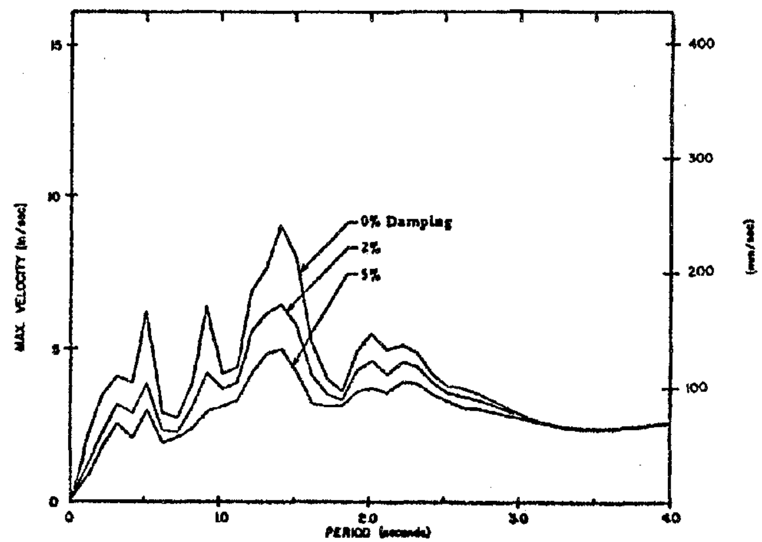

Fig. A24 Velocity Response Spectrum
Initial 10 Seconds, Parkfield E/Q. 6-27-66
Cholame-Shandon Array No. 12, N50E Component

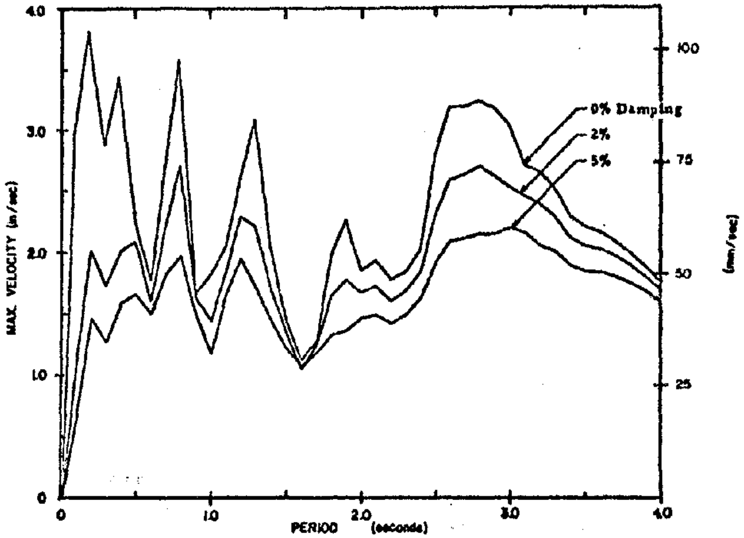

Fig. A25 Velocity Response Spectrum
Initial 10 Seconds, Parkfield E/Q, 6-27-66
Cholema-Shandon Array No. 12 Vertical Component

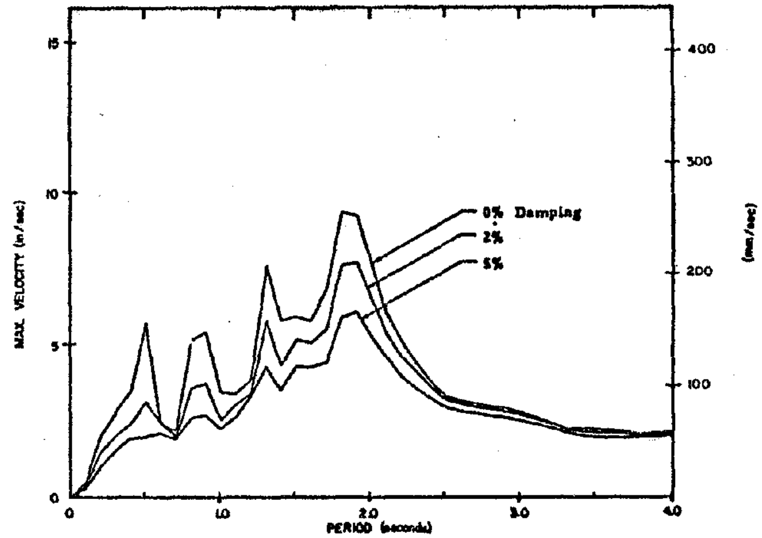

Fig. A26 Velocity Response Spectrum
Initial 10 Seconds, Artificial Accelerogram A-1

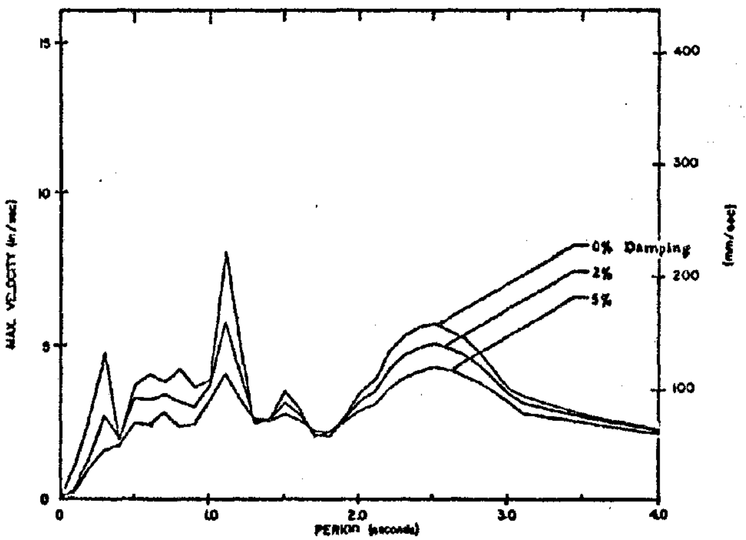

Fig. A27 Velocity Response Spectrum
Initial 10 Seconds, Artificial Accelerogram A-2

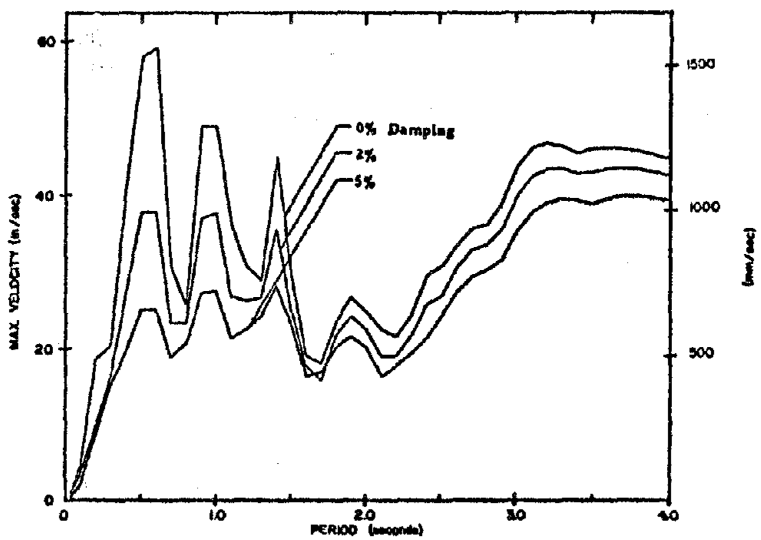

Fig. A28 Velocity Response Spectrum
Initial 10 Seconds, Artificial Accelerogram B-1

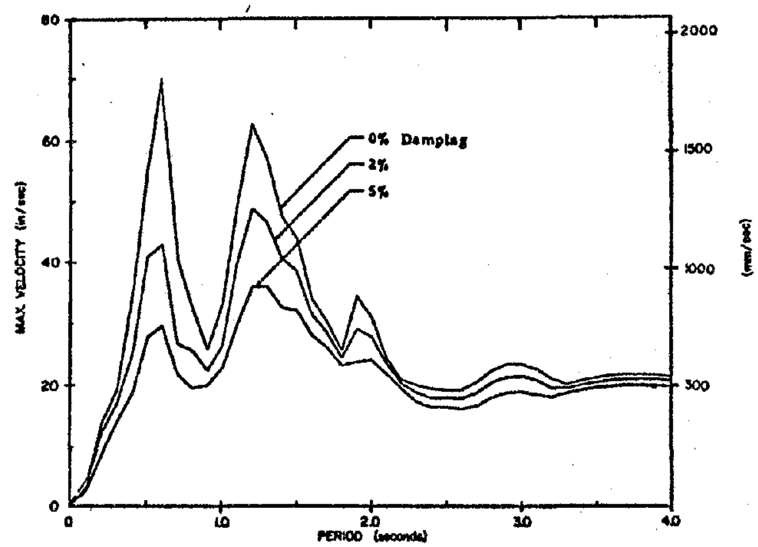

Fig. A29 Velocity Response Spectrum
Initial 10 Seconds, Artificial Accelerogram B-2

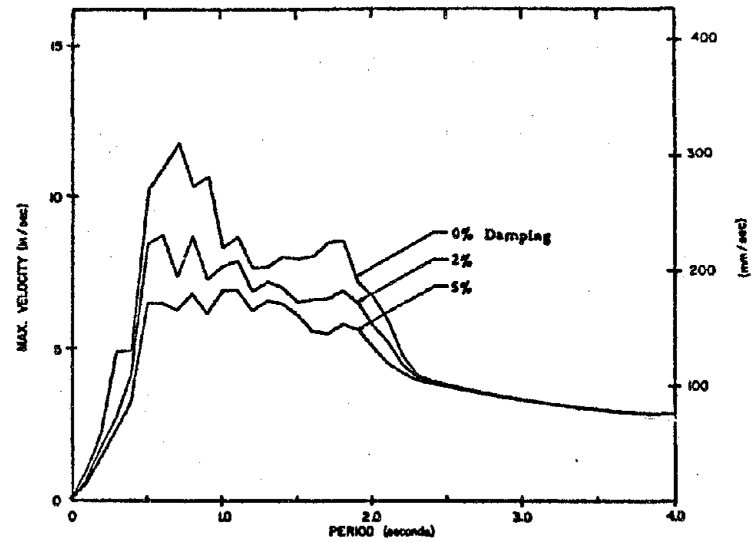

Fig. A30 Velocity Response Spectrum
Initial 10 Seconds, Artificial Accelerogram C-1

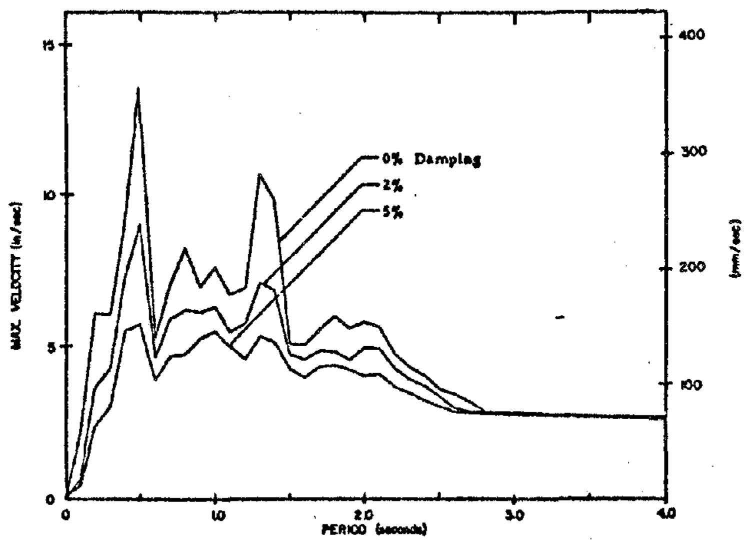

Fig. A31 Velocity Response Spectrum
Initial 10 Seconds, Artificial Accelerogram C-2

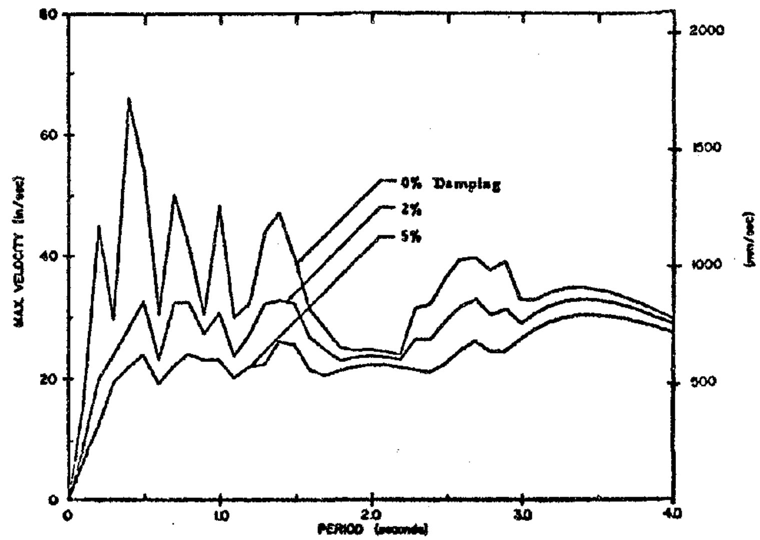

Fig. A32 Velocity Response Spectrum
Initial 10 Seconds, Artificial Accelerogram S1

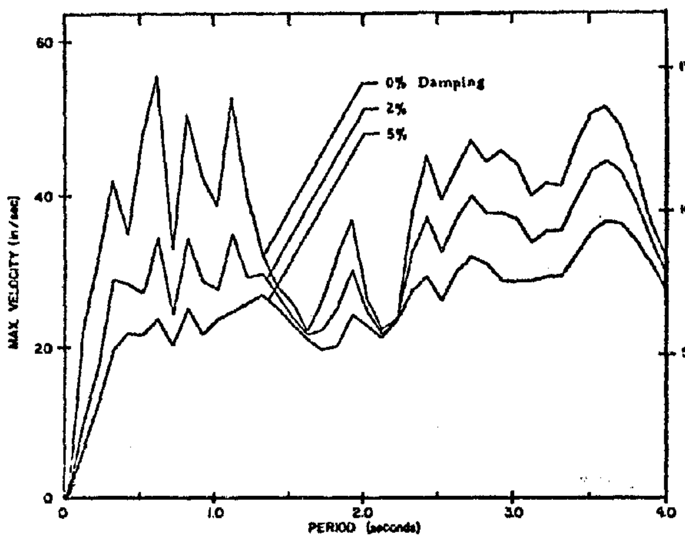

Fig. A33 Velocity Response Spectrum
Initial 10 Seconds, Artificial Accelerogram S2

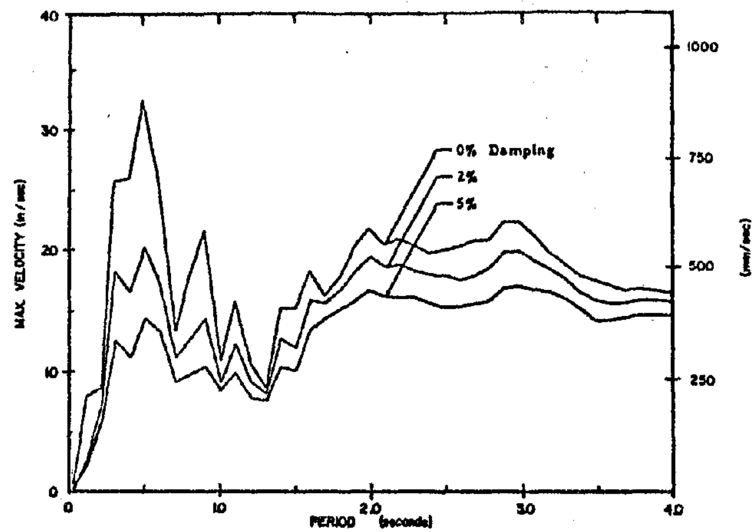

Fig. A34 Velocity Response Spectrum
Initial 10 Seconds, Artificial Accelerogram S3

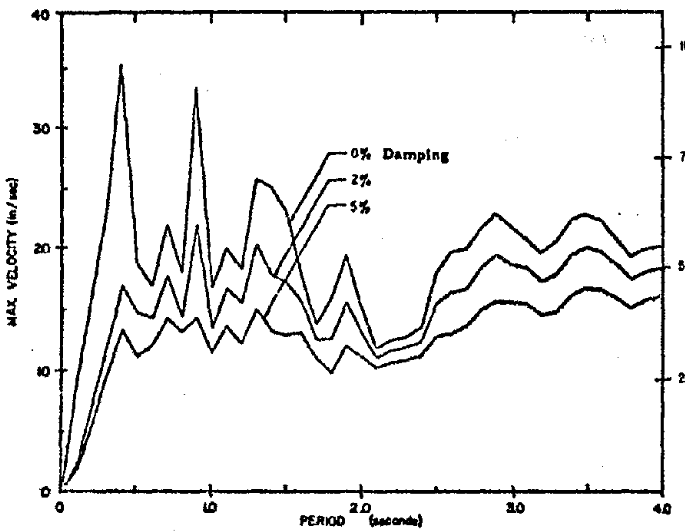

Fig. A35 Velocity Response Spectrum
Initial 10 Seconds, Artificial Accelerogram S4

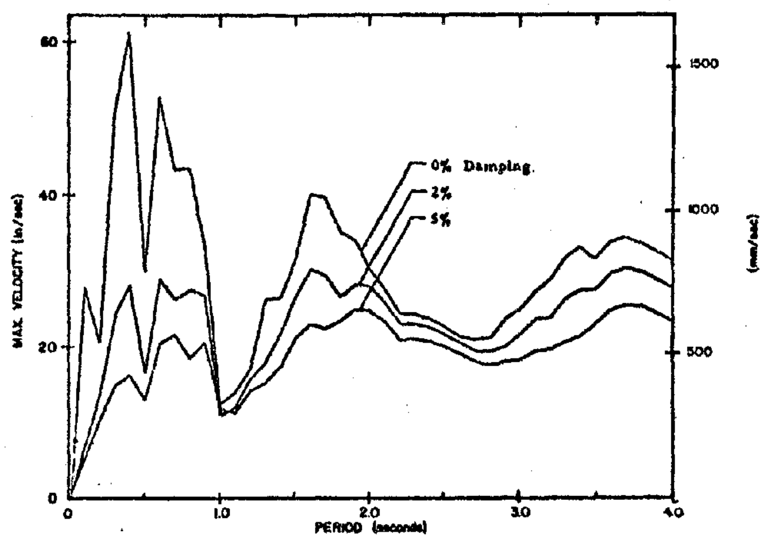

Fig. A36 Velocity Response Spectrum
Initial 10 Seconds, Artificial Accelerogram S5

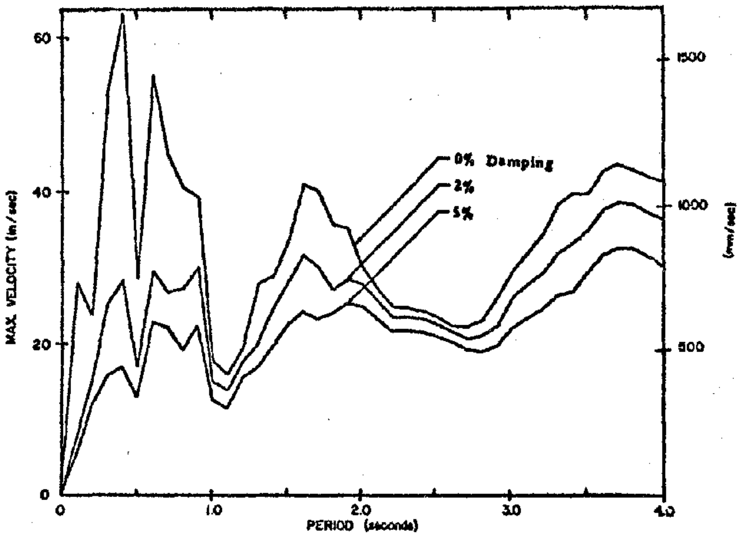

Fig. A37 Velocity Response Spectrum
Initial 10 Seconds, Artificial Accelerogram S6

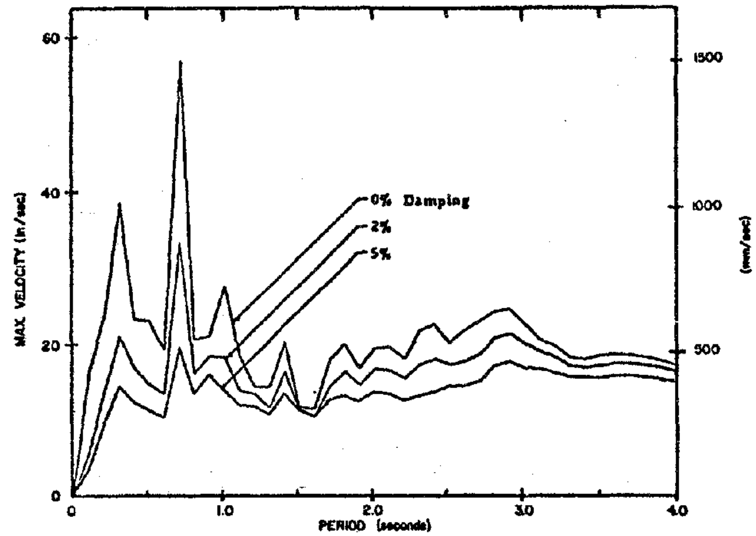

Fig. A38 Velocity Response Spectrum
Initial 10 Seconds, Artificial Accelerogram P1

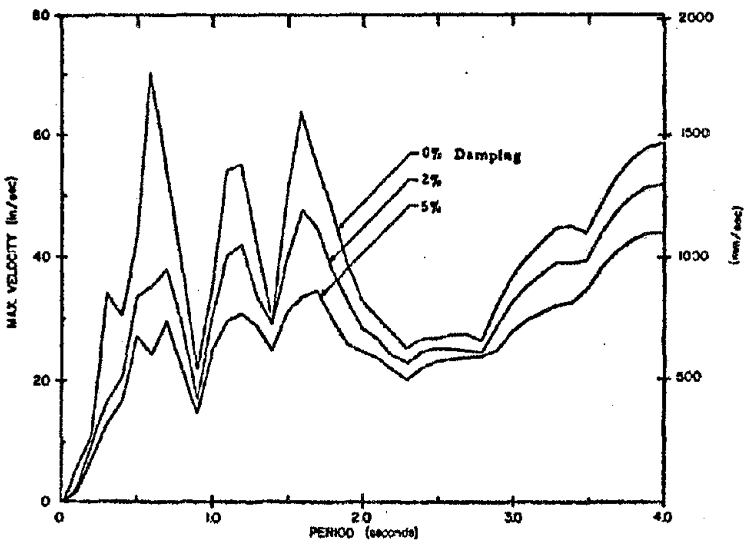

Fig. A39 Velocity Response Spectrum
Initial 10 Seconds, Artificial Accelerogram P2

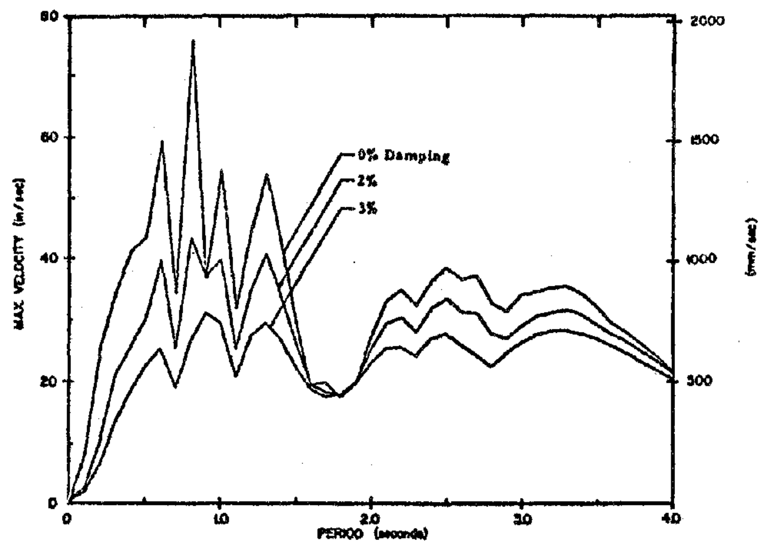

Fig. A40 Velocity Response Spectrum
Initial 10 Seconds, Artificial Accelerogram P3

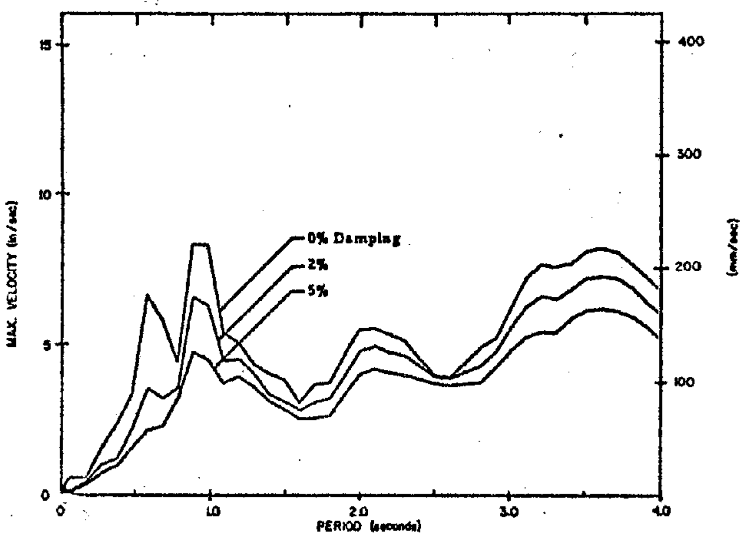

Fig. A41 Velocity Response Spectrum
Initial 10 Seconds, Artificial Accelerogram P4

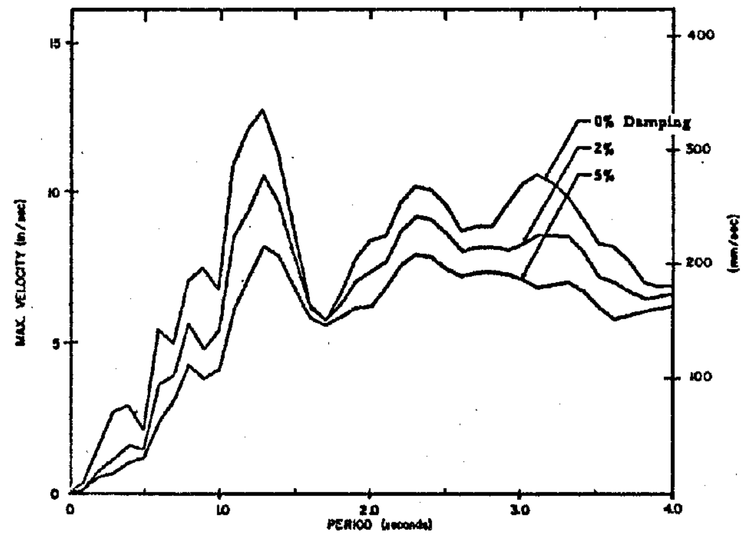

Fig. A42 Velocity Response Spectrum
Initial 10 Seconds, Artificial Accelerogram P5